MARKARIAN 501 MONITORING CAMPAIGN USING ROVOR

by

Richard L. Pearson III

A senior thesis submitted to the faculty of

Brigham Young University

in partial fulfillment of the requirements for the degree of

Bachelor of Science

Department of Physics and Astronomy

Brigham Young University

April 2010

BRIGHAM YOUNG UNIVERSITY

DEPARTMENT APPROVAL

of a senior thesis submitted by

Richard L. Pearson III

This thesis has been reviewed by the research advisor, research coordinator, and department chair and has been found to be satisfactory.

_____   _____
Date   J. Ward Moody, Advisor

_____   _____
Date   Eric Hintz, Research Coordinator

_____   _____
Date   Ross Spencer, Chair

ABSTRACT

MARKARIAN 501 MONITORING CAMPAIGN USING ROVOR

Richard L. Pearson III

Department of Physics and Astronomy

Bachelor of Science

The remote telescope facility of Brigham Young University, ROVOR, observed
Mk501, a variable blazar, for over 60 nights. These observations took place
from April 2009 to March 2010. Possible microvariability ($\Delta t \simeq 10$ to 30min)
was found in three nights, thereby limiting the size and mass of the central
black hole within Mk501. No periodic behavior was identified, but intranight
variations occurred daily. SBP photometry, a new reduction method, was
first used to analyze the Mk501 data. However, the method requires a larger,
brighter object; M81 was therefore observed and SBP photometry was per-
formed to prove the quality of the SBP photometry data. A variation of
0.005 ± 0.001mag was found over a period of 2-minutes, thus verifying the
usefulness of this reduction method. Additionally, tools to help with ROVOR
operation are included.

ACKNOWLEDGMENTS

Contents

List of Figures

Chapter 1

Introduction

Billions of galaxies have been found in the known universe [1]. Though each galaxy is generally unique, many similarities exist. Edwin Hubble originally distinguished between "Regular" and "Irregular" galaxies. He divided the "Regular" galaxy group into *ellipticals* and *spirals* [2]. Further classification studies have helped to further define these galactic groups and has "facilitated the process of trying to understand the nature of galaxies" [3]. Additional projects, such as the one presented here, help add a considerable amount of data regarding galaxy variability. Background information pertaining to variable galaxies and an overview of the project at hand are found below.

1.1 Active Galactic Nuclei and Markarian 501

Active galactic nuclei (AGNs) describe a category of galaxies that are host to an active core, or nucleus. This active core emits high-energy radiation. Seventeen years after the first discovery of an active galaxy in 1908 by Edward A. Fath, Carl K. Seyfert "reported that a small percentage of galaxies have very bright nuclei" [3, 4].

Since then, further clarifications have been made to the Seyfert galaxies, including the AGN.

The AGN model consists of the active core being driven by a supermassive black-hole with an accretion disk swirling about it. The action of the accretion disk perturbs the material enough so that the closer it gets to the blackhole, the hotter it becomes. It is this material that is responsible for the high-energy emission in AGNs.

AGNs have been further divided in terms of the direction the emission jet faces (with respect to the earth). A *blazar* is a group of AGNs that has the jet facing directly toward the earth. The elliptical galaxy, Markarian 501 (Mk501), falls into this category [5]. It is one of the few known TeV blazars[1] and is relatively nearby ($z = 0.034$) [6,7]. Mk501 was chosen as the target of interest for a year-long campaign. It is relatively bright ($\approx$ 13mag) and is accessible in the sky for most of the year (RA= $16 : 53 : 52.2$, DEC= $+39 : 45 : 36.6$). The AGN model has been extended to include every galaxy in the universe. It proposes that every galaxy in the universe holds a blackhole at its center. To better confirm and clarify this presumption, a study of AGN is necessary and Mk501 was chosen for examination.

Three things were hoped to be obtained from the Mk501 observations. First, we hoped to find small, short variability in the blazar. This is otherwise known as intraday variability or IDV. Second, day-to-day (or rather night-to-night) variations, known as intranight variations, were sought. Third, periodic behavior in the IDV and intranight variability was searched for. All of these were to assist in confining the universal AGN model. The IDV and intranight variability helps constrain the size and mass of the central blackhole. The periodicity helps in better determining the physical processes occurring at the center of AGNs.

---

[1]TeV stands for a *teraelectron volt*, which is a trillion electron volts.

1.2 Photometry

The nature of the Mk501 campaign required reevaluations of the nature of charged-coupled device (CCD) calibrations. Photometry calibrations must be performed on the CCD images to obtain accurate measurements. This is usually completed by obtaining intensity readings from the images using computerized apertures, or circles defining areas to read, centered on the objects of interest. However, for extended objects like Mk501, the normal procedures (absolute and normal differential photometry) did not seem sufficient. Finding IDV and periodicities in Mk501 require smaller errors than normal photometry will allow. Using the Ph.D. thesis written by Stephen McNeil [8], we further investigate, outline, and detail surface brightness profile (SBP) photometry. Proof of the validity of this new process is included as photometry compiled on another AGN, M81. Chapter 3 describes the process and chapter 5 outlines the results of the photometry (both normal and new).

1.3 Remote Telescopes

To fulfill the goals of the Mk501 campaign, nightly observations from a good, dark site was required. Over the past two years, Brigham Young University (BYU) undergraduates have been working to build an operable remote telescope facility. The remote facility was run during the evening at a location far from city lights and BYU campus. The Remote Observatory for Variable Object Research (ROVOR) in Delta, Utah was the result.

As a co-constructor in the ROVOR facility, I have put together this senior thesis to provide most of the information one would need to operate ROVOR. It includes specialized user manuals, troubleshooting help, as well as some software and reduction code. It was, in a way, designed to be an all-encompassing user manual. Therefore,

Chapter 2 describes, in much more detail, the features of this telescope and the reason for its construction. Chapter 3 goes through the reduction and photometry techniques used for ROVOR's data. Chapter 4 walks through some definitions of statistical equations used with ROVOR and commonly found in astronomical literature. The chapter regarding the results (chapter 5), portray the excellent data of Mk501 and M81 obtained from the ROVOR site. The 70-plus nights used over the past year for scientific research (and over 60 of those nights included imaging Mk501) has established ROVOR as a fully operational remote telescope facility.

Chapter 2

ROVOR Setup

The Robotic Observatory for Variable Object Research (ROVOR) is a remote telescope facility owned and operated by Brigham Young University (BYU) (see Figure 2.1). It is stationed on a cow pasture 12 miles northwest of Delta, UT. The dark skies and coarse—but acceptable—seeing (about 3 arcseconds) provide good, quality observations. ROVOR had been under construction, constant maintenance, or manual control until its first fully robotic run on April 1, 2009. Over 70 nights have been used for scientific research since then. Uncomplicated hardware and straightforward software operate the telescope and make the operation easy. Specifics of the ROVOR setup are described here.

2.1   Hardware

Since ROVOR was to be operated and maintained by primarily undergraduate students, the hardware was chosen to facilitate this use. Most of the hardware came with off-the-shelf software, providing relatively fluid communication and operation. Other hardware was designed and created by BYU faculty with the same users in mind.

Figure 2.1 An outside view of the Robotic Observatory for Variable Object Research (ROVOR) in Delta, Utah. The main telescope is housed in the larger building (the dog-house), while the computer controls are held in the smaller building (the outhouse).

ROVOR is housed within the Lifferth Dome, a facility designed and constructed by Wes H. Lifferth of the Physics-Astronomy Department at BYU. The dome cover is completely removed before telescope operation, providing three specific benefits: no need to operate through a slit, horizon-to-horizon viewing, and a simple open and close. The first and third benefits allow for straightforward communication and operation. The horizon-to-horizon viewing allows the telescope to track any object in the viewable sky with relative ease, making many of the projects associated with ROVOR feasible. Since the telescope sits high in the building, a set of mercury switches, attached to the telescope mount, prevent the dome from closing (or opening) if the telescope is in a hazardous position.

The telescope itself is a 16-inch RC Optical tube situated on a Software Bisque Paramount ME (see Figure 2.2).[1] This German equatorial mount allows the telescope to easily track diurnal objects, which are objects that move with the general motion of the stars. However, the equatorial mount requires the telescope to change sides

---

[1]The telescope is technically a RCOS Carbon Truss 16-inch Ritchey-Chrétien Telescope.

Figure 2.2 A view of the RC Optical System telescope, used at the ROVOR site.

of the meridian when it tracks objects through the meridian.[2] Slight mechanical pointing limits are acquired with this feature, but the software packages eliminate this drawback.

A charge-coupled device (CCD) and filter wheel are attached at the back end of the telescope. Two CCDs have been used the past two years. First was a 1k x 1k Apogee Ap47 camera which provided a 0.7375 arcsec pixel^{-1} resolution and a 12 x 12 arcminute field of view (FOV)[3]. The current CCD is a 1k x 1k Apogee Ap8 camera in a Finger Lakes Instrumentation (FLI) body and gives 1.35 arcsec pixel^{-1} resolution and a 22 x 22 arcminute FOV.

In front of the CCD, six filters are held in a FLI filter wheel: B, V, R, I, 'wide' and 'narrow' $H\alpha$. A description of the sensitivity of each filter can be found in Dr. J. Ward Moody's ROVOR files.

---

[2]The meridian is the imaginary line that runs directly through due-North to due-South, through the zenith. The zenith is the imaginary point directly overhead.

[3]For the project described here, the Ap47 CCD was used in a binned mode, or a binning of the pixels 2-by-2. This essentially doubled the plate scale from 0.735 to 1.475 arcsec/pixel. Though it limits the minimum spatial resolution, it was sufficient for the Mk501 campaign presented here

2.2   Software

As stated previously, the hardware and software were selected to make operating ROVOR relatively simple. Also, many of the hardware pieces were supplied with off-the-shelf software making communication between the telescope, the computer, and the programs rather smooth.

2.2.1   Software Bisque Packages

Much of the hardware uses programs released by Software Bisque (SB). The mount, CCD, and filter wheel operate by the following programs: `TheSky`, `CCDSoft`, `Orchestrate`, and `TPoint`. Though each program can be run individually and manually, when ROVOR is used robotically, these programs communicate with one another almost seamlessly. A brief discussion regarding the functions of each program and future improvements regarding software operation is given here. More information and specialized ROVOR operation manuals are included in Appendix D.

`TheSky` displays a virtual nighttime sky, set at the telescope's location. Within this program, the telescope is parked (i.e. placed at the position where the telescope rests when not in use), homed (slewed to the default position where the telescope encoders are reset), and directed throughout the night.

`CCDSoft` controls the CCD and filter wheel. It is responsible for maintaining the CCD temperature , changing filters, adjusting the telescope focus, and taking images. Appendix D includes further specifics regarding initial setup, download times, filename saving, and temperature limitations.

`Orchestrate` is the scripting software for all of the SB applications. In `Orchestrate` itself, one compiles an automated script which sends commands to the telescope, camera, and filter wheel. There are many nuances particular to this software and many

of them are included in Appendix D for reference. But even though it is not the easiest and most user-friendly package, it has helped make ROVOR a truly remote and (somewhat) robotic telescope. To help create nightly scripts, an additional graphical user interface (GUI) is being constructed. The GUI will wrap around `Orchestrate` and run it in the background. Through it, the user will be able to more easily construct nightly scripts to be sent to ROVOR.[4]

The `TPoint` software is used quite rarely, but holds some of the most important information regarding the operation of the telescope. The sole purpose of the `TPoint` package is to correct telescope pointing errors. One may think that if great care were taken to properly align the mount and balance the telescope, then no corrections should be needed. However, the guiding precision necessary for untrailed images is one part in 15 million and no gears are machined that precisely.[5] `TPoint` is used to analyze and remove this pointing error by building a "TPoint Model". Details on producing a model and its use can be found in Appendix D. Once the model is completed, it runs in the background of `TheSky` as `TheSky` operates the mount and telescope. If, for some reason, the `TPoint` model does not seem to correct the pointing error enough, SB also produces an additional program to take out periodic error fluctuations (for an additional $100.00), called `Precision PEC`. We have not found the need to purchase this software; `TPoint` has performed excellently.

The commercial, off-the-shelf software from SB continues to operate ROVOR. Since working out most of the kinks in the communication and hardware interface, the software has given little resistance to nightly observations. Still, further improvements

---

[4]This idea sprouted in March 2010 with Bret Little (currently and undergraduate). He was at the head of the interface construction.

[5]If—in assembling the mount and telescope—the alignment was off by only a half-a-degree, the error in the telescope pointing would equivocally be 30 arcminutes; thus, the object of interest would most likely be found outside of the telescope's FOV.

can be provided; a GUI wrap-around program for `Orchestrate` or a purchase of SB's `Precision PEC` are a couple of suggestions.

2.2.2 LabView Programs

LabView is a very powerful and useful graphical programming language. Before the renovation of ROVOR (which upgraded ROVOR to the features found in §2.1 and §2.2), students put together a main control terminal for the original mount and telescope using LabView. Currently, LabView is only used for one simple, important action: the dome operation.

A National Instruments data acquisition (DAQ) device is powered through a USB connection with the computer. It sits on the wall of the outhouse with wires from the dome control box in the doghouse attached to its I/O leads. The program that currently operates the dome is entitled "MainControl". Additionally, this program displays the weather station's text file and a screenshot of the infrared camera.

Though LabView has made it quite easy to compile these needed operations, the program uses a large amount of the central processing unit (CPU) on the computer. When LabView is running, the time it takes for CCDSoft to download images during an observation run is increased by about 40% (it takes about 8 seconds to download an image without LabView running and almost 12 seconds with it running). It will be necessary in the future to create another method for displaying the current weather and perhaps an even simpler program to open and close the dome.

2.2.3 Weather Station

The software to run the weather station was put together by Daniel E. Wilcox, a BYU alum. Once it is running from `dos`, two text files are output: one text file is a

complete record of the day's weather; the other file is continuously updated (currently, every 30 seconds). The latter file is read into the LabView program as described in §2.2.2. Further details are found in Appendix C.

Chapter 3

Reduction and Photometry Techniques

Calibrating CCD images to collect statistically viable photometry is an art of error minimization. A CCD image is an array of photosensitive wells that convert incoming photons into electrons. The electrons are counted by an analog-to-digital (A/D) amplifier and reported as *counts* (a really technical name). However, the wells within the CCD do not distinguish between photons; photons arriving from a celestial object, a flashlight, a random cosmic ray, or any other source are not differentiated on the CCD. This is where the art of reduction comes into play.

To provide good photometry from the desired celestial object, all other possible forms of light (or photon counts) need to be accounted for and removed. A series of calibration frames are used to remove the unwanted photons. Following the reduction, photometry calculations are performed on the object of interest. This section describes the various types of calibration frames, the programs used for reductions, and two types of CCD photometry. Also, Steve B. Howell's book, entitled "Handbook of CCD Astronomy" is one of the best resources and is highly recommended

(it's actually a fairly nice read) [9].

3.1 Calibration Frames

A CCD image is a collection of object light, a bias level, and background noise or light by pixels of varying sensitivity. This can be expressed as a simple equation:

$$\mathbb{R} \times \phi + \mathbb{D} + \mathbb{Z} = \mathbb{I}, \tag{3.1}$$

where $\mathbb{I}$ is the raw, unprocessed frame initially from the CCD; $\mathbb{R}$ is the real light from the object of interest; ϕ is the individual pixel variation; $\mathbb{D}$ is the background noise; and $\mathbb{Z}$ is the bias level. Calibration frames are taken to understand the contribution of each term. Note that different types of astronomical work require a slightly different "image equation" (i.e. Equation 3.1) and thus, different types of calibration frames. For ROVOR, an optical telescope without a spectrometer, the calibration frames are of three types: biases or zeroes, darks, and flats.

3.1.1 Biases

An electronic offset is applied to CCD data so the A/D amplifier operates linearly at low light levels. This offset is measured by a bias, or zero, frame which is essentially a zero-second exposure image with the shutter closed. The purpose of this is to simply read each pixel's *biased* level. To remove this bias level from the raw, unprocessed image, one simply directly subtracts the bias frame from the raw frame. Therefore, Equation 3.1 now becomes

$$\mathbb{R} \times \phi + \mathbb{D} = \mathbb{I} - \mathbb{Z}. \tag{3.2}$$

A good practice is to collect a large amount of bias frames, average them together, and subtract them from the raw image. When these are averaged, it is wise to use a

min/max rejection. This throws out the minimum and maximum values associated with each pixel throughout all the frames. This then helps reduce the error in each pixel and eliminates random cosmic ray hits.

3.1.2 Darks

A dark frame is a measure of the random noise level surrounding the CCD. It accounts for things such as hot pixels, CCD temperature gradients, and thermal stability. The dark frame is taken with the shutter closed, but with the same exposure times as the object frames. For example, if you are exposing for 90 seconds on a particular object, then you will want to collect a series of 90 second darks. Because the darks collect random fluctuations, it is usually a good idea to take the average (again, usually with a min/max rejection) of many frames to use in a dark correction. For ROVOR, we have found it good practice to take a large number of darks at the beginning and end of an observing night, along with a few throughout the night.

Darks must be obtained at the same temperature as object frames as well, since the thermal fluctuation counts are proportional to the temperature of the CCD. Note that the dark frame itself is a combination of a bias level and the noise. Therefore, the dark frames need to have their bias subtracted out as well. The bias subtraction needs to happen before the darks are averaged together. After the bias has been subtracted from the darks and the darks have been averaged together, the dark counts can be removed from the bias-subtracted raw frame, simply by subtraction:

$$\mathbb{R} \times \phi = \mathbb{I} - \mathbb{Z} - \mathbb{D}. \tag{3.3}$$

Remember that the $\mathbb{D}$ here has been bias-subtracted as well. If you find that subtracting the bias from the dark actually causes more error, you can just use the averaged dark frame for subtraction, with the bias level still "intact". For my research, this is

the process that I used. We found that with the previous CCD (the Apogee 47p), it was best to use a collection of dark frames without the bias subtracted from those frames. So, instead of having $\mathbb{I} - \mathbb{Z} - \mathbb{D}$, we used the form $\mathbb{I} - \mathbb{D}z$, where $\mathbb{D}z$ was the dark that had not been bias-subtracted; mathematically, you can see, these two equations are essentially equivalent. The latter, however, did not include an averaging of the bias level. We hoped that by leaving out the bias averaging, the statistics would improve (we did not run any test to determine if this statistically improved the photometry; all we know is that it did not make it worse).

One last thought regarding dark subtraction on the new, current CCD (the FLI version of an Ap8). We have been running the CCD at a temperature of $-30\,^{\circ}C$. This provided excellent images and fine photometry. However, we found that the CCD could go down to $-45\,^{\circ}C$. By doing so, a 60 second dark frame had the same counts as a bias frame, thereby eliminating the need for the dark subtraction (because $\mathbb{D} - \mathbb{Z} \simeq 0$). This is common for cryogenically cooled optical CCDs, whose temperature gets to about $-100^{\circ}C$; the thermal noise (due to heat) is no longer present and dark frames are not used. I strongly suggest to begin working the CCD at $-45\,^{\circ}C$. Though it is not as cold as $-100^{\circ}C$, diminishing the dark variance would help improve the quality of the resultant data.

3.1.3   Flats

The flat frame, or flat field, is designed to find out how each individual pixel varies when exposed to light. The CCD manufacturer tries—and the cost per CCD is usually directly related to the quality of the CCD—to make each pixel react the same to incoming photons. However, imperfections exist and must be handled; hence, the flat field.

The idea behind the flat field is to expose every pixel on the CCD with the same

number of photons, or the same intensity of light. If you know that each pixel is receiving the same amount of light, then the variations from pixel to pixel will be a measure of their sensitivity. Some pixels will be brighter and others will be dimmer. By normalizing the frame[1], each pixel will have its own weight factor (in Equation 3.1, ϕ is the pixel's weight factor). If the bias-dark-subtracted image is then divided by the weight factors, pixel-to-pixel, the real light from the objects is found:

$$\mathbb{R} = \frac{\mathbb{I} - \mathbb{Z} - \mathbb{D}}{\phi}. \tag{3.4}$$

There are further calibrations completed on the desired science objects during the photometry process, but those only come after the completion of the reduction process, or the division of the normalized flat field.

Obtaining a flat field is a fairly tricky process that still has flaws within it. They are possibly the most error-prone images you will ever take. The best flat field frames are obtained by pointing the telescope about 5 to 10 degrees from the zenith, just after sunset or just before sunrise. We assume that the images we take at this part of the sky at this time of night equally illuminates the CCD, giving every pixel the same amount of light. It is best to obtain frames that hover around $20,000$ peak counts for optimum signal-to-noise. This typically means that flat frame exposures run from 1 to 5 seconds. Therefore, flat frames do not need any dark subtraction; they only need to be bias subtracted. And, just like the other calibration frames, the best idea is to collect a large number of frames then min/max-average them together. However, you will need to obtain flat frames for each filter, because each filter changes the specific frequency of light that interacts with the CCD. This is a crucial part of flat fielding.

Additionally, because the ROVOR telescope is settled on an equatorial mount, the CCD image flips $180\,^{\circ}$ when crossing the pier. This means that the flat fields will

---

[1]Normalizing an image involves taking the average value of the frame and dividing the frame by that average. This makes the frame average nearly equal to 1.

look different when the telescope is on the west of the pier as compared to on the east side. Therefore, both west and east flats are necessary. We found that performing both morning and evening flats—with west flats taken at night and east flats taken in the morning—works fairly well. This does mean that careful planning is needed when creating an automated script to ensure proper beginning and ending times. Though a bit tedious, this provides quality images for photometry.

3.2 `IRAF` and `Mira`

There are two astronomical programs that are used at BYU: IRAF and `Mira`. Each has their strengths and weaknesses. Some have even found it useful to do the reductions in `Mira` and the photometry in IRAF. Regardless how they are used, both programs are powerful and helpful.

The Image Reduction and Analysis Facility, or IRAF, is a more cryptic but powerful tool than `Mira`. It only runs on Linux machines (there is a Linux computer room in the astronomy department). It has been tested and used by many astronomers; so much so, that in most scientific papers, the phrase, *"Standard IRAF procedures were used"*, is quite common. Instructions on how to operate IRAF are not included here, but is left to the Observational Astronomy courses. Rather, the program is presented here to acknowledge its existence and powerful analysis features. However, none of the reduction or photometry for this project was completed in IRAF for reasons explained below.

Mira is another off-the-shelf program that was used in this project (see chapter 2). Though not as powerful as IRAF, `Mira` was chosen to be consistent with the off-the-shelf idea. This overall idea was to run a remote telescope facility with off-the-shelf hardware and software to allow for easy operation and smooth data reductions. `Mira`

runs on Windows computers and allows for personalized scripting. It is also much more user-friendly than the command-line IRAF and therefore easier for a beginning astronomy student to reduce ROVOR data.

Two advantages of `Mira`—that the ROVOR group found—is its easy reduction methods and simple program scripting; specific instructions for both can be found in the `Mira` help folder.[2]

Many of the procedures that were used for this particular project were completed using specialized `Mira` scripts. The source code for each of the procedures is found on the ROVOR computers, along with a description of the use of the program. A lot of time was taken to create scripts that could be easily used (and altered) in the future.

3.3 Photometry

Photometry is used on CCD images to analyze the photon count provided by the image. There are two ways to do photometry: absolute and differential. Absolute photometry consists of imaging two fields throughout much of a very *photometric* night (a night that is perfectly clear, with no high cirrus clouds or highly variable seeing). The object of interest is imaged, then followed by imaging a standard star field. These fields have been observed and standardized. The standardization provides a constant base where objects of interest can be compared. The standard field stars are taken to be constant so that the object of interest can then be compared

---

[2]The scripting language that `Mira` uses is called the *Lua language*. It is described from its online reference manual as "an extension programming language designed to support general procedural programming with data description facilities. It also offers good support for object-oriented programming, functional programming, and data-driven programming. Lua is intended to be used as a powerful, light-weight scripting language for any program that needs one. Lua is implemented as a library, written in clean C (that is, in the common subset of ANSI C and C++)" [10].
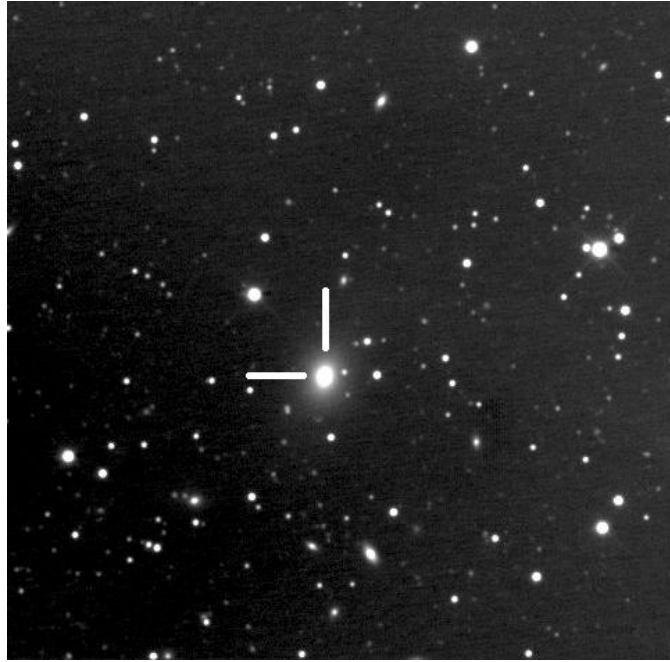
Figure 3.1 Markarian 501 (Mk501), as viewed from the ROVOR site. This elliptical galaxy is classified as a blazar, with a redshift of $z = 0.334$.

against the constant to look for variation. For more information regarding standard photometry techniques, see [11, 12] and reference therein. As an extension of those standard fields, other stars are standardized in other fields. Differential photometry uses these secondary standards as comparison stars. Having these secondary stars in the field of view (FOV) around an object of interest permits observations to occur on not-so-perfectly photometric nights. Differential photometry was used in this project in order to maximize the imaging time with ROVOR. Two variations of differential photometry were attempted for this project: surface brightness profile photometry and normal differential photometry.

3.3.1 Surface Brightness Profile (SBP) Photometry

Normal differential photometry works well with point source objects, or stars. The method has draw-backs once the point sources become extended objects. This project

focused on one extended object, namely Mk501 (see Figure 3.1), an elliptical AGN. The problem with extended objects and normal differential photometry is that the other stars are quite far away from the point of interest on the object. The point of interest is the center region of the elliptical galaxy—the black hole emission jet region. Because the stars are so far away from the center of Mk501 (and other extended objects in general), flat fielding errors are amplified. To overcome this, McNeil studied the use of surface brightness profiles (SBPs) on extended objects to obtain differential photometry [8]. Instead of using surrounding stars as a constant standard, the bulge of the galaxy (or extended object) is used as a reference. Two separate images, and their respective SBP bulges, are used to compare the magnitude of the central region. The difference in the two SBPs should be the differential magnitude of the central region. The process is described below and follows the steps outlined in the simple list form of Table 3.1.

Step 1

After reductions have been completed on the object frames, an important decision needs to be made. The SBP photometry requires both a reference or comparison image and an object image. The reference image can be the subsequent image from the object frame or it can be a combined image of 20-60 images. The combining of images to create a reference frame helps improve the photon statistics; however, it also smears the PSF of the reference image, which degrades the statistics. Having a combined image reference frame also allows you to use the reference frame for multiple nights, so that each individual object frame is being compared to the same reference frame through the whole campaign. The benefit of using the subsequent image allows a direct image-to-(next)image comparison, and therefore minute-by-minute variations throughout the whole night (and campaign). The former idea was chosen for this

Step	Description	Comment
1	Decide on a reference frame	Use a combined or single image
2	Match images' PSFs	
3	Get counts ($\mathcal{C}$) inside concentric circles	Usually from radius of 1 to 12 pixels
4	Calculate the cnts/annulus ($\mathcal{C}_n$)	Do this by subtracting the inner counts; see §3.3.1
5	Calculate the cnts/ann/area ($\mathcal{C}_{nA}$)	Divide value from Step 4 by area of annulus ring
6	Compute the magnitude/area (m_{nA}) for each radius	Use $-2.5\log(\mathcal{C}_{nA})$
7	Perform steps 3 - 6 for second image	
8	Plot values from Step 6 (the m_{nA}) vs. radius for each image	This is the SBP
9	Align the bulge light of the two SBPs	see §3.3.1 for more details
10	Convert the new, adjusted m_{nA} (m_{nAadj}) back into $\mathcal{C}_{nA}$	Use $10^{-0.4 m_{nAadj}}$
11	Sum up $\mathcal{C}_{nA}$ in each SBP	
12	Find differential magnitude	Use $-2.5\log(\frac{\sum \mathcal{C}_{nAref}}{\sum \mathcal{C}_{nAobj}})$

$\mathcal{C}$	=	counts within an aperture
$\mathcal{C}_n$	=	counts within an annulus
$\mathcal{C}_{nA}$	=	counts within an annuls per area
m_{nA}	=	magnitude within an annuls per area
m_{nAadj}	=	adjusted magnitude within an annuls per area
$\mathcal{C}_{nAref}$	=	adjusted counts within an annulus per area in the reference image
$\mathcal{C}_{nAobj}$	=	counts within an annulus per area in the single object image

Table 3.1 Steps for SBP photometry, with explanatory chart of variable terms.

(a) A radial profile of a star's PSF.
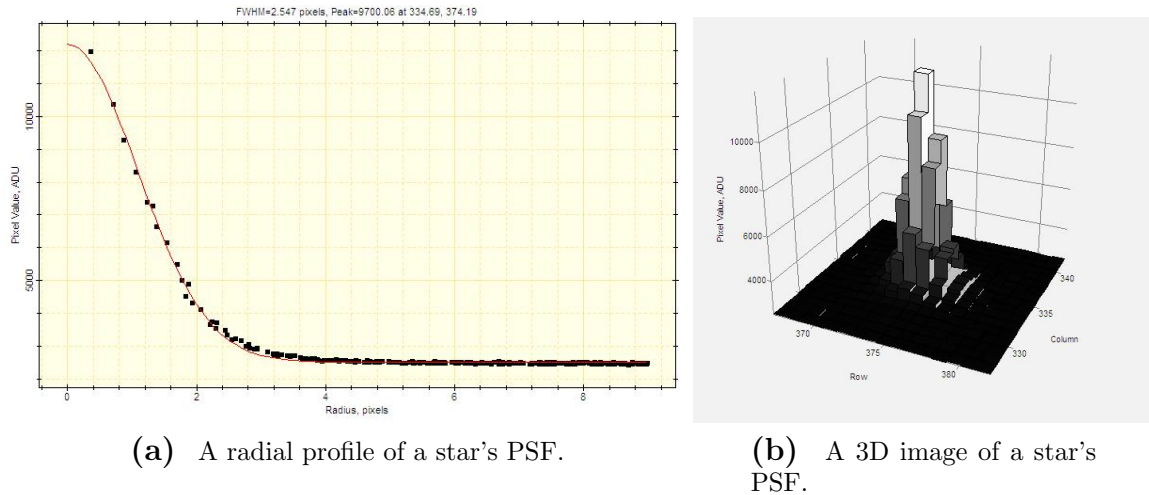
(b) A 3D image of a star's PSF.

Figure 3.2 Images of a single star's PSF. An average of many star's PSF (across the whole CCD) becomes the image's PSF. The PSF is recorded as a FWHM of a gaussian profile

particular Mk501 project, by combining 60 images from May 28, 2009.

Step 2

Once the reference frame decision has been chosen, the next step is to make the two images' PSF the same. The significance of this step cannot be fully impressed. The PSF determines how much the incoming light is spread onto the CCD. A point source (a regular star) creates a gaussian profile on the CCD (see Figure 3.2). By having the PSFs matched, variable seeing effects and defective flat fielding effects are greatly diminished. However, if the PSFs are incorrectly matched, false variations will be reported in the photometry. The `Mira` program actually reports the FWHM of the PSF and that is what is used to find the PSF of the image itself. IRAF can also provide a PSF template; directions on how to do that can be found in the form of Dr. Hintz or Physics 529 (or a little bit of 329).

The PSF matching was done using `Mira`'s FWHM scripting commands. The script references the use of another program, only used for this one purpose. It is called

`MRMaterials`, the "MR" standing for multi-resolution [13]. Only one command is used: *im_simu*. The program itself is quite large and the commands run through the `dos` system. Every new computer that the program runs on needs a special license file. I have communicated with Dr. Murtagh (the creator of the software) through the ROVOR email address (rovor.byu@gmail.com) to obtain new license files for new computers. Continue to do this in the future if the need arises. The application as well as licence file must be in the working folder with the images that are being processed. The easiest thing to do is to copy the licence and `exe` file into each new working folder and then run the PSF fitting script. Simply, the *im_simu* command takes an image and then convolves that image with a gaussian PSF of a specified input width; this varies the images' own PSF. The script calls this command, remeasures the image PSF, then performs the convolution again if needed. The user specifies the PSF error, but a difference in PSF's of about 0.00002 is typical (and quite good!). The convolving takes about 30 loops, if the initial width is a good guess. This script makes life a lot easier and provides sufficient results.

Step 3

Following the matching of the PSFs, photometry measurements can begin without worrying about the PSF matching errors. The photometry measurements will be used to build up the SBPs for each image (the reference and object frame). To do this, we find the total counts within a user-defined aperture ($\mathcal{C}$). The aperture is simply a circle centered about the maximum point of light on an object. The $\mathcal{C}$ within that region are then summed and reported. To create SBPs, apertures of varying radii are compiled together. McNeil went from 1 to 10 pixels in increments of 0.5 pixels; for this project, we went to 12 pixels with increments of 1.0 pixels. We chose to do this because of ROVOR's larger plate scale (1.375 and 1.475 arcsec pixel^{-1}) as compared
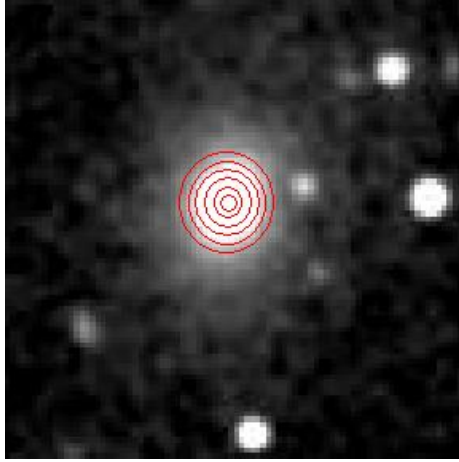
Figure 3.3 An example of the collection of apertures, superimposed on top of Mk501. The annulus' that these apertures make are used to create SBPs. See §3.3.1 for more details.

to the plate scale used by McNeil ($\approx$0.3 arcsec pixel^{-1}) [8].

Usually, there are two other larger circles defining a ring, or annulus, for "sky" subtraction. However, this project replaced the values in the sky annulus with another method. Areas surrounding Mk501 were chosen as vacant and empty regions on the CCD; these are defined as "sky areas". The counts in these regions were averaged together to find an average pixel value of the sky background. That value was then subtracted, pixel-by-pixel, across the whole frame. Therefore, the sky subtraction still occurred, just not with the sky annulus.[3]

---

[3]The reason for this change was again due to the fact that we were working with an extended object. Because there is no definitive place where the galaxy light ends, placing an annulus for background subtraction might include some of the galaxy light itself. To be safe, we decided to go with this procedure. Performing the subtraction this way is actually quite similar to the process used to calibrate photometers (see [14]). Standard procedure would be to observe the star, then observe the black, empty sky nearby. This would ocurr throughout the night. Part of the reductions would then include subtracting the background sky noise counts from the star's counts. Now that CCDs can image a whole area of the sky at once, choosing these dark, empty areas can be easily found and used for sky subtraction.

Step 4

After $\mathcal{C}$ has been retrieved from each aperture, we must find the counts in each annulus, or $\mathcal{C}_n$. The various sized apertures create a bullseye-target when superimposed on the object (Figure 3.3). The annulus, or ring, is defined as the area between two apertures. The SBPs are created with the counts found in each annulus. To get the counts in each, one simply subtracts the counts of the inner aperture from the counts of the outer aperture. As the apertures increase in radius, the number of counts within the aperture will increase; the resultant of the subtraction will be a positive number. Note that the most inner aperture acts as its own annulus. Mathematically, it looks like the following:

$$C_n = C_i - C_j. \tag{3.5}$$

Here, i and j are integers denoting the radius of the aperture, where j ranges from the minimum radius to one less than the maximum radius ($r_{min} \leq j \leq r_{max} - 1$) and $i = 1 + j$.

Step 5

After each $\mathcal{C}_n$ has been found, we can now produce the counts area^{-1}, or $\mathcal{C}_{nA}$, calculation for each annulus. This simple calculation divides the counts in each annulus (the $\mathcal{C}_n$ found in Step 4) by the area associated with that annulus. The area of the annulus is determined by subtracting the area of the two apertures (the same apertures used to determine the annulus counts or the areas of i and j). Because the apertures are round circles, the simple geometric equation of the area of a circle is used: *Area* $= \pi r^2$. *The radius used in the area calculation is in arcseconds.* To convert from pixels to arcseconds, multiply the aperture radius by the plate scale of the CCD. For example, in the case of the Ap8 CCD that is currently down at ROVOR,

radii of 1 pixel = 1.475", 2 pixel = 2.95", 3 pixel = 4.425", and so on. Then, the

annulus area (A_n) is just,

$$A_n = A_i - A_j \tag{3.6}$$

$$A_n = \pi \left(r_i^2 - r_j^2 \right), \tag{3.7}$$

where r_i is the radius of the large aperture and r_j is the radius of the small aperture.

Then, Equation 3.5 can be used with Equation 3.7 to find the counts area^{-1} in each

annulus:

$$\mathcal{C}_{nA} = \frac{\mathcal{C}_n}{A_n} \tag{3.8}$$

$$\mathcal{C}_{nA} = \frac{\mathcal{C}_i - \mathcal{C}_j}{\pi(r^2 - r_j^2)}. \tag{3.9}$$

The resultant values for each annulus are used to create the SBPs after converting

them into magnitudes, as shown next.

Step 6

To create the SBPs, we use the values found from Step 5 to compute a magnitude.

Using the magnitude relation of

$$m_{nA} = -2.5 \log(\mathcal{C}_{nA}), \tag{3.10}$$

where m_{nA} is the magnitude area-1 calculated from $\mathcal{C}_{nA}$ (the values computed in

Equations 3.8 and 3.9). McNeil uses the mag area-1 reference many times in his

thesis, so we continue to use it here for clarity[4] [8].

---

[4]In actuality, McNeil found a magnitude area^{-1} sec^{-1}. He divided the annulus counts by their
area *and* by the exposure length of the image. This may have been because of varying exposure
lengths between the comparison images. However, with the research presented in this senior thesis,
the comparable images had the same exposure; the division of the exposure time has been removed.
Mathematically, the exposure division was simply a constant magnitude adjustment: *mag area*$^{-1}$ =
$-2.5 \log(\frac{cnts/ann}{area} \frac{1}{exposure}) = -2.5 \log(\frac{cnts/ann}{area}) + 2.5 \log(exposure)$. Hence, the exposure was left
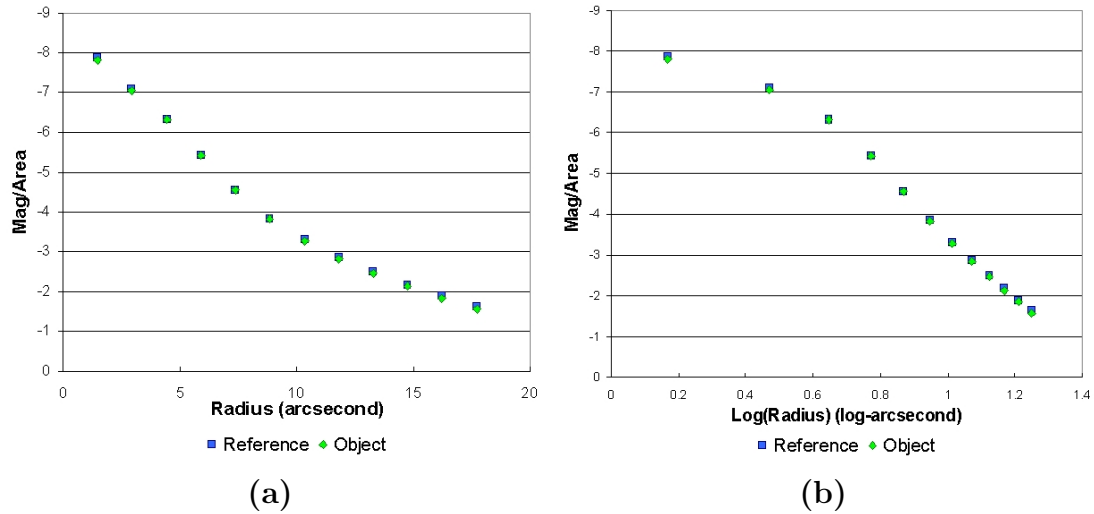out for simplicity's sake.

Figure 3.4 Examples of a SBP of Mk501. Notice that for magnitudes, the more negative, the brighter an object. Hence, the y-axis has been flipped to be consistent with brighter being up. The second image is a semi-log plot, with the x-axis a $\log(radius)$.

Step 7

If you have not already done so, repeat steps 3 through 6 for the second image. Both images' values from Step 6 will be used to perform the final differential photometry.

Step 8

We are now ready to create the SBPs for each image (the reference and object image). Both SBPs are plotted on the same plot. To form a SBP, the m_{nA} values from Step 6 are used on the y-axis with the associated radii (in arcseconds) on the x-axis. Figure 3.4a shows an example of an SBP completed on Mk501. Figure 3.4b is a plot with the $\log(radius)$ along the x-axis. This second image shows the difference in the profiles a little better than the first, regular plot. It also emphasizes the profile's trends: (a) a smooth, sloping tail associated with the bright bulge; (b) a "turning-over" curve, to where the slope is approaching zero; and (c) a brighter, central region associated

with the jet emitted by the blackhole.

Step 9

After the SBPs have been calculated and plotted, the next step is to align the profiles. At the beginning of this section, it was briefly explained that instead of using far away stars for calibration and differential photometry, we were going to use the profile of the galaxy bulge light. This bulge light is displayed as the smooth, outer portion (larger radius) of the SBP.

To align the profiles, simply subtract the m_{nA} values corresponding to the *bulge*. But, where does the bulge begin—or more importantly—where does the nucleus light end? This is a question that must be decided for each extended object observed, because they will vary. For Mk501, we felt confident in declaring that anything past 6 pixels (or about 8 arcseconds) was safe. Also, our collaborator from the University of Denver suggested an aperture radius of 7 arcseconds to be consistent with other research. We also concluded this based upon trial and error.

Once the bulge differences are found, average these difference values (from each annulus) together. Then adjust the entire SBP (each m_{nA} value) of either image with the average difference. For the example SBP (i.e. Figure 3.4), there was an adjustment of 0.039237 mag area^{-1} needed. This is denoted as a Δm_a and was applied to the reference image (as seen in Figure 3.5). Note that it does not matter which SBP is adjusted; for consistency, the reference image is chosen to be adjusted to match the object image. And remember, the adjustment is not *just* for the bulge; it is applied to the *whole* SBP, including the nucleus region of the SBP. These new, adjusted values are denoted as m_{nAadj}.
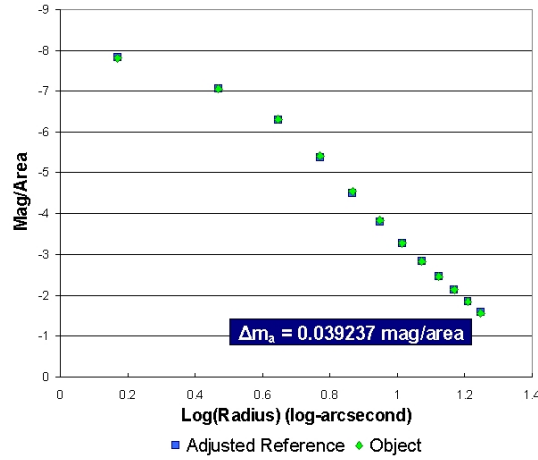
Figure 3.5 The SBP of the reference image was adjusted by the displayed Δm_a. As compared with Figure 3.4, the bulge light is almost perfectly in line. This is again a semi-log plot, with the x-axis a $\log(radius)$, used to better show small variations.

Step 10

Now that the SBPs have been aligned and matched, we convert the adjusted mag area^{-1} values (the m_{nAadj} from Step 9) back into counts area^{-1} for each annulus. To do this, we use the inverted relation of Equation 3.10,

$$10^{-0.4m_{nAadj}} = \mathcal{C}_{nAref}, \tag{3.11}$$

where the m_{nAadj} is the adjusted m_{nA} values (the value with the additional Δm_a). Therefore, the reference frames' adjusted counts area^{-1} is denoted by $\mathcal{C}_{nAref}$.

Step 11

With the adjusted magnitude conversion into counts is complete, the count values for each image are summed up separately ($\sum \mathcal{C}_{nAref}$ and $\sum \mathcal{C}_{nAobj}$). Basically, this is summing up the total counts under the SBP curve. Remember to add together the $\mathcal{C}_{nAref}$ for the reference image instead of the unadjusted counts. For the SBP example (Figures 3.4 and 3.5), the totals come out to be $\sum \mathcal{C}_{nAref} = 2659.37$ and

$$\sum \mathcal{C}_{nAobj} = 2647.27.$$

Step 12

Finally, we are now able to find the differential magnitude between these two images. To do so, we use the total counts found in Step 11 from each of the images in the following equation:

$$\Delta M = -2.5 \log \frac{\sum \mathcal{C}_{nAref}}{\sum \mathcal{C}_{nAobj}}. \tag{3.12}$$

The derivation of this equation can easily be reproduced, but will not be done here. For your interest, the SBP example that we have been following produces a value of -0.00495; this means there was a 0.00495 difference between the object and reference frames.

Care must be taken to understand the true meaning of the negative sign (or positive sign, as the case may be). If it is easier to work in magnitudes without the negative sign in front of the 2.5 (as in Equation 3.10), then take off the negative sign. Just remember that you did that when playing around with other numbers and data.

3.3.2 Normal Differential Photometry

Before continuing, a confession is necessary. After months of trying to make the SBP photometry method work with Mk501, the errors were unacceptably large. The hypothesis is that Mk501 was too small to output a decent bulge profile. However, to prove the worth and value of the method, we imaged an extended object with a larger, brighter bulge: Messier 81 (M81), a large, nearby galaxy host to an AGN (see Figure 3.6). SBP photometry was previously performed on M81 by McNeil [8]. His results for M81 are presented in Table 5.4, along with further analysis regarding the SBP photometry on M81, are found in §5.1. Therefore, much to our dismay, we had

Figure 3.6 M81, as viewed from the ROVOR site. It has a highly active nucleus in the center of its "grand design" spiral nature.

to resort to performing normal differential photometry on Mk501. A description of our methods is described in this section.

The ideas behind differential photometry and its usefulness was discussed in the introduction of the Photometry section, §3.3. To summarize, there are standard stars (assumed to be constant) in the FOV of Mk501. By imaging Mk501, the other standard stars are imaged too. Mk501 can then be compared against the unvarying standards to look for internal variations. The standards in the Mk501 field are shown in Figure 3.7.

To perform differential photometry, one aperture size is chosen for the stars and for Mk501. To be consistent with other work previously performed (as well as current collaborator assistance), we chose to work with an aperture radius of 7.375-arcseconds[5]. We opted to use a sky subtraction over the whole frame instead of a sky annulus (see

---

[5]To obtain this radius, we used $r = 5$ pixels, binned 2×2 on the Ap47p and $r = 5.463$ pixels binned 1×1 on the new Ap8.
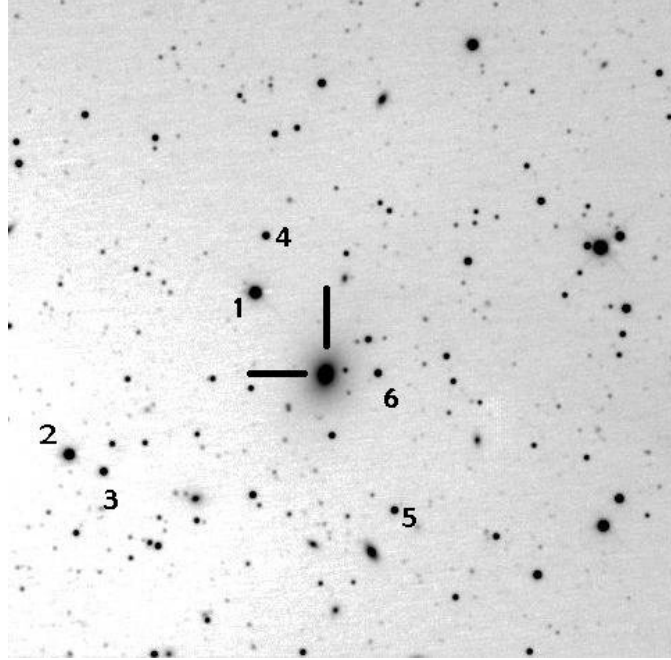
Figure 3.7 Mk501 and its associated standard stars. The numbering system was derived from the finder chart [15].

Step 3 in §3.3.1 for further details).

Once the aperture counts for Mk501 ($\mathcal{C}_{MK}$) and the stars ($\mathcal{C}_i$) were obtained, they were converted into an instrumental magnitude:

$$m = -2.5 \log(\mathcal{C}) \tag{3.13}$$

Then, the instrumental magnitudes for all the standard stars are averaged together ($m_s = \frac{\sum_{i=1}^{N} m_i}{N}$, where N is the total number of standard stars used). Finally, m_s is subtracted by m_{MK}, or the instrumental magnitude of Mk501. This difference becomes the differential magnitude, ΔM, of Mk501 in that image. The ΔM, with its smaller associated error, is used in analyzing nightly fluctuations (also known as intra-day variability, or IDV).

For long-term monitoring, m_{MK} is converted into a true magnitude. Mk501 hovers around a magnitude of 13. To convert the m_{MK}, we move back to the standard star's instrumental magnitude. Each star's magnitude is then compared to the standard

values ($m_{\mathcal{S}i}$) produced by Villata [16] and Fiorucci [17][6]. The $m_{\mathcal{S}i}$ values remain constant throughout the whole campaign. The average difference in the standard values ($m_s = \frac{\sum_{i=1}^{N}(m_i - m_{\mathcal{S}i})}{N}$) is found and then applied to Mk501's instrumental magnitude: $M = m_{MK} - m_s$). The resulting value is Mk501's true magnitude. The m_s quantity acts as a calibrated zero point that turns m_{MK} into a true apparent magnitude.

As one final note, the error associated with ΔM is only a combination of the Poisson statistics associated with Mk501 and its nearby standards. On the other hand, the latter magnitude calculation introduces further error associated with the standard star calibrations. In fact, the ΔM error is about 10 times smaller than the error in the true apparent magnitude. This is why the simple differential magnitude is used for IDV detection. When reporting long-term monitoring values, the error associated with the true magnitude is not as significant and is evident in the plots within Chapter 5.

---

[6]Cameron Pace, a graduating senior at BYU, is creating standard values for more stars to be used in calibrations such as these. See his senior thesis and upcoming publication(s) for more detail [11]

Chapter 4

Error Analysis

As stated in the introduction of Chapter 3, the point of photometric reductions is to minimize the error associated with the results from each CCD image. To minimize error, a brief description regarding statistical mechanisms is required; the art of error minimization is an understanding of photometry statistics and error sources. This chapter describes an overview of some basic statistics commonly used in astronomy and specifically, photometry. Additionally, some sources of the error inherit in CCDs are discussed. Also, statistical measurements regarding photometric error are presented.

4.1   Overview

The need to minimize and report error in scientific experiments is fundamental in presenting quality data-sets. In astronomical photometry, there are a number of commonly reported statistical measurements. These include the error per observation (or standard deviation), the error of the mean (or standard deviation of the mean), the signal-to-noise ratio (S/N or SNR), and many others. This section presents some

details of a couple of those statistical measurements, not full derivations or comprehensive explanations. Additional information can be found in general statistic books [18, 19] as well as specific engineering and scientist statistic references [20, 21]. Only discussions concerning standard deviations, SNR, and AGN microvariability tests are presented here.

4.1.1 Standard Deviation

The standard deviation per observation, σ_{obs}, is a measure of the average deviation of a set of values from the sets' mean. In the case of astronomical photometry, σ_{obs} represents the average deviation of a set of magnitudes (of a particular object) from the mean magnitude value of the set. The equation described for σ_{obs} is given as:

$$\sigma_{obs} = \sqrt{\frac{\sum_i^N (m_i - <m>)^2}{N}}.$$

(4.1)

In this equation, N = number of images, $<m>$ = average magnitude of the N images, and m_i = magnitude in a single image. This is useful in determining the general deviation in a set. For the Mk501 campaign, the σ_{obs} was only used to determine the deviation from the average on a given night as well as the SNR (see §4.1.2). This helped determine if the night included microvariations. Other than that, the σ_{obs} was not used during this project (though it helpful to know what it is and what to do with it for analyzing other papers and results).

You will find that some report the equation above with an $(N - 1)$ in the denominator instead of the N. The reason for this is based on statistical theories and personal preference. Those ideas, however, are not described here. For the Mk501 campaign, Equation 4.1 was sufficient for its use.

4.1.2 Signal-to-noise Ratio

The SNR is a significant piece of an image's observational error. It takes into account the sky noise, CCD readout error, CCD photon-to-electron conversion (the gain), and the Poisson error in the count measurement. The readout noise and gain errors are discussed in §4.2.1. In summation, the gain accounts for the number of electrons that are produced with one incoming photon. It would be ideal if the relationship was 1:1, but it is not and the SNR tries to account for that mismatch. Here is the SNR equation, in all its glory [22, 23]:

$$\frac{S}{N} = \frac{C_{obj}}{\sqrt{\frac{C_{obj}}{G} + o\sigma_{sky}^2 + o\frac{\sigma_{sky}^2}{p}}} \tag{4.2}$$

This equation assumes that the sky counts have already been removed from the object. Section 3.3 goes through the sky-removal process. Therefore, C_{obj} = true object counts; G = gain; o = pixels in object aperture; p = pixels used for sky count calculation; and σ_{sky} = standard deviation in the sky count calculation. As can be seen in this equation S is the signal from the object (the numerator on the right-hand side) and N is the noise in the object signal (the denominator on the right-hand side).

To explain further, the σ_{sky} is the standard deviation (see §4.1.1) of the counts in the sky aperture. As noted in 3, there are two ways to calculate the sky counts: using larger apertures for a "sky annulus" around the object, or selective dark areas around the CCD frame. The latter option was chosen for this project. An average counts/pixel value was obtained for each area; then each area value was averaged. This became the sky background value for the particular CCD image. Additionally, the standard deviation was calculated for each area and averaged to become the σ_{sky} for each frame. Both the subtracted sky value and sky standard deviation are placed into the header as values in "SUBBACK" and "SUBBACKE".[1]

---

[1]More recent reductions put these values into "SKYCNTS" and "SKYERR".

Lastly, the o and p are the total number of pixels used in determining the object's counts and the sky's counts, respectively. For the circular aperture around the object, the o is just the area of the aperture. The p is the total number of pixels used in all of the selected dark areas; for Mk501, we used 6 boxes with 100 pixels in each box. Therefore, $p = 600$.

To convert the SNR value from error in counts to error in magnitude (σ_{SNR}), a relatively simple relation is used. Recall that conversion to a magnitude is

$$\sigma_{SNR} = -2.5 \log C. \tag{4.3}$$

If the C value represents the ratio of $\frac{S+N}{N}$ (or $\frac{S}{N} + 1$)—which is the ratio between the "noisy" signal and the deviation in the noise—then the σ_{SNR} can be found. This is a relatively simple calculation to perform, once S and N have already been found. There are simplifications that can be performed to make the transition simpler, but they lead to further uncertainty in the true error (for example, the simplest simplification is that $\sigma_{SNR} \simeq 1/(S/N) = \frac{N}{S}$) [23, 24]. A simple calculation in a `Mira` script or `Excel` sheet takes care of the processing headache, so a more accurate calculation is easy.

One final, additional note. Before I found this equation, I thought that an SNR calculation was simply the ratio of the total signal (C_{obj} in the SNR equation) to the sky background value (the header value of "SUBBACK"). I could not have been more incorrect. The SNR value is the ratio of C_{obj} to the *uncertainty* in the sky background, relative to the object. For quick estimations, if $S \gg N$, then Equation 4.2 turns into $\frac{S}{N} \simeq \sqrt{S}$. This is the simple error estimation of Poisson statistics. But again, do not use the actual counts divided by the sky value for your SNR value.[2]

---

[2]In Howell [9], he expresses the S/N ratio as $C_{obj}[C_{obj} + o(N_{sky} + N_{dark} + N_{readout}^2)]^{-\frac{1}{2}}$. The new terms are defined as follows: N_{sky} is the number of photons per pixel from the sky contribution; N_{dark} is the number of *electrons* per pixel from the dark subtraction; and $N_{readout}$ is the number

4.1.3 Propagation of Error

The propagation of error is an important concept in statistics. It is a more accurate and precise way of stating statistical errors. For example, if there were two numbers, each with an associated error, a simple (less accurate) way of calculating the resultant error would be to add the error values together. For better accuracy, one would add the error values "in quadrature". This means to take each error, square the value, add the squared value to the other squared errors, then square-root the result. An example of a series of errors added in quadrature is the noise value in the SNR equation (Equation 4.2). Each term (in the denominator) is a squared error value that are added to another (the first term is actually the square of a square-root, $\sqrt{x}^2 = x$). This concept is important in finalizing photometric errors and is described more fully in §4.3.

4.1.4 AGN Microvariability Tests

There have been a number of statistical tests produced for analyzing variability in AGNs. However, only the variability confidence parameter was used in this Mk501 campaign. Nevertheless, the rest are briefly described here so that when future analysis of the data occurs, these tests will be readily available. The tests were constructed to look for intraday variability (IDV), or microvariability over an evening of observation. Three of the most significant are the *variability confidence parameter*, *IDV amplitudes*, and *structure functions*.

---

of *electrons* per pixel from the readout noise. Howell expresses that each form of the S/N equation reveals the same conclusions, so each is alright to use. This was just to help in understanding of the other errors associated with the S/N equations.

Variability Confidence Parameter

The variability parameter applied to AGN is described in a number of sources [25–28]. This parameter, which we will define as $\mathfrak{C}$, is defined as a level of confidence in the IDV. Basically, it finds the variation of data points throughout the night in relation to the error, or the σ. It assumes that differential photometry is being used; this means that there is a designated comparison star and a check star (see §3.3.2). By definition, the $\mathfrak{C}$ parameter is

$$\mathfrak{C} = \frac{\sigma_{\Delta M}}{\sigma_{\Delta stars}}. \tag{4.4}$$

The $\sigma_{\Delta M}$ is the observational error in the differential magnitude of Mk501 (or any AGN), as defined in §3.3.2. The $\sigma_{\Delta stars}$ is the observational error in the differential magnitude between the comparison and check stars. If $\mathfrak{C} \geq 2.576$ then the difference is real at a 99% confidence level. (The 2.576 falls out of the statistical percentage value of a normal standard deviation distribution [18].)

This confidence parameter was not used extensively in the current Mk501 project due to the omittance of a check star. Instead, a stellar average, assumed to be constant was used to find Mk501's differential magnitude. However, recent calculations may necessitate the additional usage of single comparison and check stars. More details are described in the Differential Photometry section, §3.3.2, as well as the Data section, §5.1.

IDV Amplitudes

The measurement of IDV amplitudes coincides with the confidence parameter in the previous section: once $\mathfrak{C}$ is determined to be greater than 2.576, then the amplitude of the IDV is calculated. This parameter measures, basically, the percentage of the

night that is above 2σ. The equation is [25, 27]

$$A = \frac{100}{< \Delta M >}\sqrt{(M_{max} - M_{min})^2 - 2\sigma^2}, \qquad (4.5)$$

where A is the IDV amplitude, $< \Delta M >$ is the average differential magnitude of that particular night, M_{max} is the maximum differential magnitude, with M_{min} as the minimum magnitude. The σ represents the averaged error over the course of the night [28]. If we were to use this equation for the Mk501 project, the σ would be the average of the frames' error, from each night ($\frac{1}{N}\sum \sqrt{(\sigma_{SNR})^2_{Mk501} + (\sigma_{SNR})^2_{star}}$). §3.3.2 explains the error associated with each Mk501 image.

Obviously, the larger the amplitude, the more confident you will be that there is in fact IDV occurring. The same is true for a high confidence value, $\mathfrak{C}$. However, caution must be taken to closely look at the differential magnitude light curves for each night. Many AGN scientists not only plot the differential magnitudes of the object, but also plot the comparison star's differential magnitudes (the magnitude difference between the comparison star and the check star) [29–31]. In this way, they can determine if the variability seen in the object is truly inherit in the object or not. Equations 4.4 and 4.5 help enumerate and solidfy the IDV trends.

Structure Functions or Duty Cycles

Structure functions, sometimes referred to as duty cycles, is another analytical way of searching for small-scale variation, flares, and/or periodicities in AGN. It is out of the scope of this senior thesis to completely describe every feature, derivation, and equation relating to the structure function. However, this is a very useful tool that should be used in further analyzing active galactic lightcurves.

The simplified equations and conclusions shown here are found in Anders A. Jensen's thesis [32]. There are many additional papers that describe and use the

structure function on AGN data (e.g. [25, 27, 28, 31, 33]. A detailed study of these sources should help in better comprehending the usefulness of the structure function in searching for microvariability and periodicities.

The simple structure function equation is

$$SF = < [F(t) - F(t + dt)]^2 > \tag{4.6}$$

where $F(t)$ is the flux of the object at time t and $F(t + dt)$ is the flux of the object at a later time dt ($<>$ denotes the average of the inner quantity). This function can be used for each night's data as well as the data over a large number of days. Examples of structure functions are displayed in Figure 4.1. There are many important features that show up in structure functions. A list of these features (from Jensen [32]) are as follows:

- **Maximums** in the SF are characteristic timescales. A characteristic timescales is the "minimum time intervale in which microvariability can be detected."

- If there is a periodicity in the lightcurve of an AGN, then in the SF it is displayed as a **minimum**.

- A SF can show multiple maximums (and therefore multiple characteristic timescales). Also, only one maximum can be seen in the SF if there happened to be a bright flare in the data. Be cautious to fully rely on the SF to find the characteristic timescales.

- If calculating the SF for a series of nights, the SF will display the aliasing or windowing of the data. For instance, if data from 10 consecutive nights are used to calculate a SF, the SF will show a periodicity of about 1 day, or the time separating the large chunks of data.

- If a minimum, or periodicity, is detected at long timescale in the SF, and the minimum *follows* a maximum, it could simply be a result of a flare.

The point of the SF is to look for characteristic timescales and periodicities. It helps to further quantify the lightcurves of the AGN.

As a side note, there is a program that is used in the BYU astronomy department (and many others) called `Period04`. It is used primarily for periodic star studies (such as δ Scuti variables) but it may also be a good program to try. It "extracts the individual frequencies from the multiperiodic content of time series" that contain data gaps [34]. Whatever method is used, finding microvariability limits and periodic behavior is the core of AGN monitoring.

4.2   CCD Imperfections

It seems that everything constructed by humans contains some sort of imperfection. Even the optics on the ground-breaking Hubble Space Telescope had major issues when first put into orbit [35]. The CCD's used for other scientific research are no exception. Some of these CCD glitches include gain and readout noise, quantum hysterisis, ghosting, and many others. These listed will be discussed in further detail here.

4.2.1   Gain and Readout Noise

The gain and readout noise on a CCD are introduced in during the manufacturing process. Each value varies with filter because of the variation in the intensity of incoming photons. There were two different CCDs used for the Mk501 campaign and each of those cameras have their own gain and readout noise levels. The measurements for each of the CCDs are presented in Table 4.1.
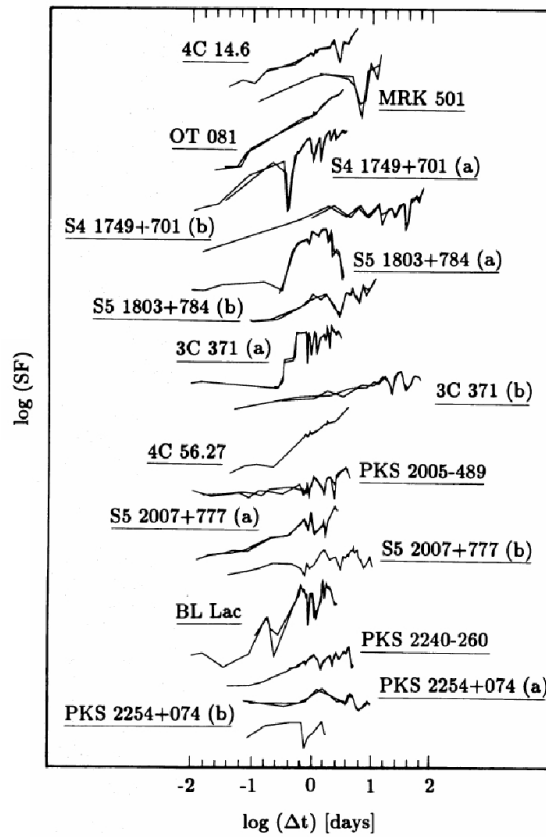
Figure 4.1 This shows examples of structure functions, SFs, of many blazars. Note the maximums and minimums of each function. The SF for Mk501 is second from the top. Image obtained from Figure 5 in Heidt and Wagner [25].

Filter	Gain (e⁻/ADU)	Readnoise (e⁻/ADU)

Filter	Gain (e$^-$/ADU)	Readnoise (e$^-$/ADU)
Ap47p (old)		
B	2.86	5.18
V	1.69	3.07
R	1.15	2.09
Ap8 (new)		
B	3.46	11.89
V	4.52	15.54
R	3.01	10.36
I	4.50	15.48

Table 4.1 This table displays the values of the gain and readout noise associated with each of the CCDs used in the Mk501 campaign. Additional details regarding each CCD is found in the Hardware section, §2.1. The ADU is another term for counts or even photons. These values were calculated by Professor Alberto Sadun, a collaborator from the University of Denver. Email correspondences are found in the rovor.byu@gmail.com address.

The gain is simply a scale factor used by an "analog-to-digital" (A/D) converter. The scale factor is there to pump up the analog signal enough so that the A/D converter can "resolve it into a range of values that can be handled by a computer" [24]. It basically determines how sensitive the AD converter is to the flow of electrons being produced by the photons. Ideally, the ratio between electrons and photons would be 1; in other words, the A/D converter would be good enough to resolve 1 electron for every 1 photon.

The readout noise arises in a CCD when the counts in a pixel move through the circuity in order to be digitally recorded. This noise, or error, accounts for the

amplification scale in the gain, the actual movement through the circuit, and the speed of the movement. Steve B. Howell states that "[a]mazing as it seems, the readout speed, and thus the rate at which currents flow through the on-chip amplifier, can cause thermal swings in the amplifier temperature, which can affect the resulting read noise level" [9]. He continues to explain that a CCD with a slower readout time generally produces lower noise levels. This is easily seen in Table 4.1. The noise levels are 2 to 5 times larger on the new CCD than the old one. Let us briefly examine these pros and cons. The purpose for changing out the old CCD with the new CCD was three-fold. First, the old CCD, the Ap47p, took about 20-30 seconds to download each image, in 1×1 binning. When we started using 2×2 binning, the download time moved to 12-15 seconds. The new CCD, the Ap8, downloads images in 5-7 seconds. Theoretically, we could produce about twice as many images on any given night. Realistically, we obtained about 1.5 times as many images. It specifically helped with remotely obtaining flat fields (which are constricted by the quickly setting sun). Secondly, the Ap8 has a FoV of about 23×23 arcminutes, whereas the Ap47p has a 12×12 arcminute FoV. The larger FoV enabled more stars in the field for comparison. It also allowed images of larger AGN to fit fully on the CCD frame. Lastly, and I think most importantly, the new Ap8 can get colder. As discussed in §3.1.2, a cooler CCD has less dark current and smaller pixel fluctuations. The Ap8 has no problem holding its own at $-45°C$, while the Ap47p was peaking at $-30°C$.

However, when the change of CCDs occurred, there were some things lost. The most significant and important difference in CCDs was the large discrepancy in the gain and readout noise levels. In the science that we are performing with ROVOR, the larger gain and readout noise contributes very little to the photometric error. As stated previously, the Ap47p had 2 to 5 times better noise levels. In the S/N equation, these noise levels are wrapped up in the σ_{sky} terms. Therefore, if the object's signal,

C_{obj}, is large enough, a 2 or $5 \times \sigma_{sky}$ won't make that much difference. For Mk501, $C_{obj} \geq 50000$ counts, with some of the comparison stars reaching over 100000 counts in the photometry aperture. Now if there comes a time where the S/N ratio decreases, the increased gain and readout noise levels will become quite significant.

4.2.2 Ghosting and Quantum Hysteresis

Ghosting and quantum hysteresis are less discussed imperfections of CCDs. The reason I have chosen to discuss them here is that we have found that both the Ap47p and Ap8 exhibit these properties.

Ghosting is charge that lingers on the CCD. If an image of a fairly bright star is recorded, the next exposure will show a remnant of that star. Its like looking at the bright sun for a second and then as you blink, the image of the sun reappears in your vision. Just as the ghost-sun in your eyes is a little detrimental to your sight for a while, ghost-stars increase photometric error of images. Extra photons are being added to the image that should have been cleared with the transfer of the previous image. Richard D. Crisp has spent much time reviewing the effect of ghosting [36, 37]. In fact, the proper scientific term for ghosting is *residual bulk image*, or RBI. Crisp wrote an article for SPI-IS&T Electronic Imaging regarding how to manage the residual bulk image [37].

For ROVOR's cameras, RBI was analyzed specifically on the Ap47p.[3] To try to account for the ghosting effects, we began imaging a bias and a dark about every 20 minutes throughout an observing night. This helped account for the extra counts in the images (because they would also show up on the darks). This did not eliminate the problem, but it helped reduce its effects during photometric calculations. By analyzing the dark and bias images, we concluded that the RBI did not horribly

---

[3]The Ap8 is discussed in a minute. Just hold on.

effect our results, leaving $\simeq$ 10's of counts; this is on the order of the gain and readout noise. The ghosting on the Ap8 was quite similar to the Ap47p. Therefore, we concluded RBI to be an additional—but not significant—source of error for both CCDs.

As for quantum hysteresis (QEH), defined as the random (or non-linear) variations associated with the signal transfer, the Ap47p may experience some symptoms [38]. We did not spend time on descriptively identifying the complete QEH signature for the CCDs. Rather, when we saw that the RBI error was sufficiently low, as well as the gain and readout noise, the effects of QEH were ruled insignificant as well. Again, it is something to take note of for future reference.

4.3 Photometric Error

Even if all of the instruments and optics on a telescope system are perfect, errors in observation and calibration factor in. These errors are caused by atmospheric effects (seeing, transparency, etc.) and pure error limitations. The latter is a built-in error to the standardization process as described in §3.3. However, differential photometry generally provides lower errors as compared to absolute photometry. Further explanation of each are described below. *Note that the values stated for σ_{tot} in both types of photometry come from the data processed for the Mk501 campaign using the ROVOR telescope.*

4.3.1 Absolute Photometry Error

To briefly summarize, absolute photometry consists of looking at the object of interest, then slewing to a standard star field. Moving back and forth between the two fields allows for comparison between the object of interest and the standardized stars.

Using transformation equations derived from the standardized star fields, a true magnitude is collected for the object of interest. Even though this is ideal, the process requires "photometric nights" in order to observe. A "photometric night" allows an astronomer to assume that the sky is acting the same in one area as another. This stability is needed in order to compare one part of the sky to another part. Though photometric nights come relatively rarely, they are the most pristine.

In context of error, the error found intrinsically within absolute photometry is based on the original standardization fields (associated with specific types of filters). The error claimed with the production of the standardized fields is typically around ± 0.01 mag (see [39] for specifics). Those original fields have been expanded to include more standard star fields; in the optical region, that expansion was completed by A. U. Landolt (see [12] for an example of his work). The errors in these expanded fields still tend toward the ± 0.01 mag level. Therefore, when using absolute photometry, in addition to the error in collecting the data (the S/N, or SNR, value), an error in comparison is added. Using the knowledge of propagating errors (§4.1.3), a total error, σ_{tot} can be calculated:

$$\sigma_{tot}^2 = (\sigma_{SNR})_{obj}^2 + \sigma_{standard}^2. \tag{4.7}$$

Here, the first term is the S/N of the object of interest (from Equation 4.3) and the second term is the error associated with the transformation using the standardized fields. For further information regarding these transformation errors (which typically come out to $0.01 - 0.03$ mag), see the senior project completed by Cameron Pace [11]. The resultant σ_{tot} falls around $0.02 - 0.04$ mag. The error value usually satisfies projects looking at long term variability. However, when searching for variability on the timescales of minutes to hours, where the variability is on the order of 0.02 mags, the high σ_{tot} values will be no good. Another solution is needed.

4.3.2 Differential Photometry Error

Differential photometry is a useful alternative to absolute photometry. It uses the magnitudes of the stars surrounding the object of interest on a CCD frame. By finding the difference between the stars and the object of interest, a "differential magnitude" is obtained for the object of interest. Also, stars within an object of interest can be standardized and used as further extensions from the original standardized fields (see previous section). This allows astronomers to work on "non-photometric" nights because variations across a single CCD frame are assumed to be constant. This allows for more obtainable (even if slightly worse) data.

By using differential photometry, one (generally) lowers the error associated with the final product. Therefore, it is used to find small amplitude variations in objects, such as Mk501. The error is depleted because differential photometry removes the intrinsic standard error (the $\sigma_{standard}$ in §4.3.1). In other words, the standard values and error are not used to re-calibrate the object of interests' instrumental magnitude. Instead, the standard stars' instrumental magnitudes and S/N errors are compared with the objects' instrumental magnitude and S/N error. Hence, the total error, σ_{tot}, is now

$$\sigma_{tot}^2 = (\sigma_{SNR})_{obj}^2 + \sigma_{stars}^2 \tag{4.8}$$

where $(\sigma_{SNR})_{obj}$ is the S/N of the object of interest and σ_{stars} is the combined S/N values of all the stars used for comparison against the object[4]. Typically, one star is chosen as a comparison star and a second star chosen as a check star. The instrument magnitudes of the object and comparison star are used for the differential photometry (and their errors are used in the equation above to find a σ_{tot} for that frame). The

---

[4]If a group of stars are used to compute a comparison magnitude, the σ_{stars} will be the average of each star's S/N value. If the comparison magnitude is just from one star, then σ_{stars} is the S/N value of that one star.

σ_{tot} usually comes out between 0.005 and 0.01 mag, more than 10 times better than the absolute photometry.

Then, the instrumental magnitudes of the comparison and check stars are subtracted to find their differential magnitudes (again, their errors are used in the equation above to find their own σ_{tot}). These values are typically lower than the object's σ_{tot} and range from 0.003 to 0.008 (the stars are usually brighter than the object and therefore have more counts). By plotting both of the differential magnitudes, variations present in both are assumed to not be variations within the object. However, if there is a feature in the object's differential magnitudes that is not present in the comparison star's magnitudes, that feature is taken to be a real variation in the object. For blazars, these variations happen so fast and so faintly, that the smaller error in the differential photometry is essential for finding the smaller trends.

Nevertheless, a differential magnitude cannot be reported as a true magnitude. Why? Because it simply is not; the differential magnitude is a difference in instrumental magnitudes. A true magnitude is produced when the instrumental magnitude is converted into one, using standard stars with standard values. Absolute photometry does just that. But again, the σ_{tot} climbs once the standard magnitudes are used in transforming the instrumental magnitudes. You may also remember that the secondary standards (in the same field of view as the object) have been calibrated in order to transform the object's magnitude. These secondary standards normally carry even higher errors than the first extended standard fields. Some of the secondary standards have errors up to 0.09 mag. This discrepancy results from smaller telescopes performing the secondary calibrations, a lack of observations, and/or a lack of plentiful *photometric* observations. Regardless, care must be used in calculating and tracking error throughout the photometry process.

Chapter 5

Results

The Mk501 campaign was designed to locate and identify variations in this particular blazar. Three types of variations were searched for: intraday variability (IDV), intranight variation, and periodic behavior. For this campaign, we obtained many images in one night in order to find IDV. We also to monitored Mk501 for a number of months to find both the intranight and periodic variations. The following chapter outlines the observations of Mk501 over the past year and describes the conclusions drawn from the observations.

5.1 Observational Data

ROVOR was able to observe Mk501 for over 60 nights. The nights varied in quality, ranging from very photometric to fairly variant seeing (but because of differential photometry, the data is still usable, just with higher errors). We were able to observe Mk501 in the B, V, R, and I bands. Due to the nature of the project, we desired the highest signal we could get with the shortest exposure time. We decided to look for microvariability primarily in the R band. Hence, the majority of our observational

Filter	Total Nights	Total Images
B	49	584
V	49	492
R	61	3693
I	24	176

Table 5.1 Total observational nights and frames over the 2009 and 2010 campaign of Mk501, for each filter. Note the heavy emphasis in the R band. Intraday variability, or IDV, was searched specifically in the R band region.

time was devoted to R band observations (see Table 5.1). Tables 5.2 and 5.3 show the entire observational campaign.

The processed R band data for Mk501 is shown in Figures 5.1 and 5.2. The first shows the normal differential magnitudes obtained with our reductions, from April 22 to July 6, 2009. The error bars used here include the error in the standard stars when converting the instrumental magnitudes into true apparent magnitudes; these fall around ±0.02 mag. The second figure displays the R band values obtained by our collaborator, Alberto Sadun, from the University of Denver. His error bars do not include the error in the standard adjustment and range around ±0.004 mag. Also, instead of using just one frame per data point, he averaged together about five frames to get a single data point per night. His plot ranges from April 22 to July 31, 2009. Figure 5.3 shows Sadun's reductions of each band through July 31, 2009.

Obviously, the full data set has not been processed. There is still much more data to reduce and compile. The reduction was not completed for a number of reasons. First, the unsuccessful attempt with the SBP photometry put things quite behind schedule. Second, the re-analyzing of the data due to bad error calculations lengthened the time required for reductions. Third, reducing the M81 data also took more time than planned. Therefore, there is quite a bit of work available for others to pick up. The results we have, nevertheless, give sufficient results to answer our

Date (2009 UT)	Date (UT, JD)	Filter	N observations
22 April	2454943	B - V - R	20 - 11 - 11
30 April	2454951	B - V - R	80 - 40 - 40
06 May	2454957	R	165
07 May	2454958	R	195
09 May	2454960	B - V - R	24 - 16 - 121
10 May	2454961	B - V - R	24 - 16 - 121
11 May	2454962	R	223
14 May	2454965	R	45
15 May	2454966	R	45
16 May	2454967	B - V - R	15 - 15 - 90
17 May	2454968	B - V - R	15 - 15 - 225
18 May	2454969	B - V - R	15 - 15 - 225
19 May	2454970	B - V - R	22 - 15 - 90
28 May	2454979	B - V - R	15 - 15 - 180
29 May	2454980	B - V - R	15 - 15 - 133
23 June	2455005	B - V - R - I	6 - 6 - 51 - 6
27 June	2455009	B - V - R - I	8 - 8 - 8 - 8
29 June	2455011	B - V - R - I	8 - 8 - 8 - 8
30 June	2455012	B - V - R - I	8 - 8 - 8 - 8
05 July	2455017	R	7
06 July	2455018	R	178
07 July	2455019	B - V - R	10 - 9 - 152
09 July	2455021	B - V - R	15 - 9 - 165
10 July	2455022	B - V - R	15 - 9 - 134
17 July	2455029	B - V - R - I	10 - 10 - 10 - 10
23 July	2455035	B - V - R	12 - 12 - 105
28 July	2455040	B - V - R - I	8 - 8 - 8 -8
29 July	2455041	B - V - R - I	10 - 10 - 10 - 10
30 July	2455042	R	55
31 July	2455043	R	74

Table 5.2 Observational record of Mk501 throughout the 2009 and 2010 season. Observational dates displayed are all 2009, except where noted. N refers to the number of frames taken in each filter.

Date (2009 UT)	Date (UT, JD)	Filter	N observations
01 August	2455044	B - V	12 - 11
03 August	2455046	B - V - R	4 - 3 - 167
04 August	2455047	B - V - R	6 - 7 - 19
09 August	2455052	B - V - R - I	22 - 18 - 24 - 8
10 August	2455053	B - V - R - I	12 - 12 - 12 - 12
11 August	2455054	B - V - R	9 - 9 - 119
17 August	2455060	B - V - R - I	10 - 9 - 10 - 10
18 August	2455061	B - V - R - I	8 - 8 - 8 - 8
20 August	2455063	B - V - R - I	8 - 8 - 8 - 8
21 August	2455064	B - V - R - I	8 - 8 - 8 - 8
22 August	2455065	B - V - R - I	8 - 8 - 8 - 8
26 August	2455069	B - V - R - I	8 - 8 - 8 - 8
27 August	2455070	B - V - R - I	8 - 8 - 8 - 8
28 August	2455071	B - V - R - I	6 - 5 - 6 - 6
29 August	2455072	R	68
01 September	2455075	B - V - R	24 - 24 - 30
12 September	2455086	B - V - R - I	4 - 3 - 4 - 4
17 September	2455091	B - V - R	8 - 7 - 16
21 September	2455095	B - V - R - I	4 - 4 - 4 - 4
22 September	2455096	B - V - R - I	6 - 6 - 6 - 6
23 September	2455097	B - V - R - I	4 - 4 - 4 - 4
24 September	2455098	B - V - R - I	6 - 6 - 6 - 6
25 September	2455099	B - V - R - I	6 - 6 - 6 - 6
26 September	2455100	B - V - R - I	6 - 6 - 6 - 6
04 November	2455139	B - V - R	4 - 8 - 15
05 November	2455140	B - V - R	10 - 10 - 42
06 November	2455141	R	7
07 November	2455142	R	85
08 November	2455143	B - V - R	10 - 11 - 87
17 March 2010	2455272	R	15
18 March 2010	2455273	B - V - R	8 - 5 - 5

Table 5.3 Observational record of Mk501 throughout the 2009 and 2010 season. Observational dates displayed are all 2009, except where noted. *N* refers to the number of frames taken in each filter.
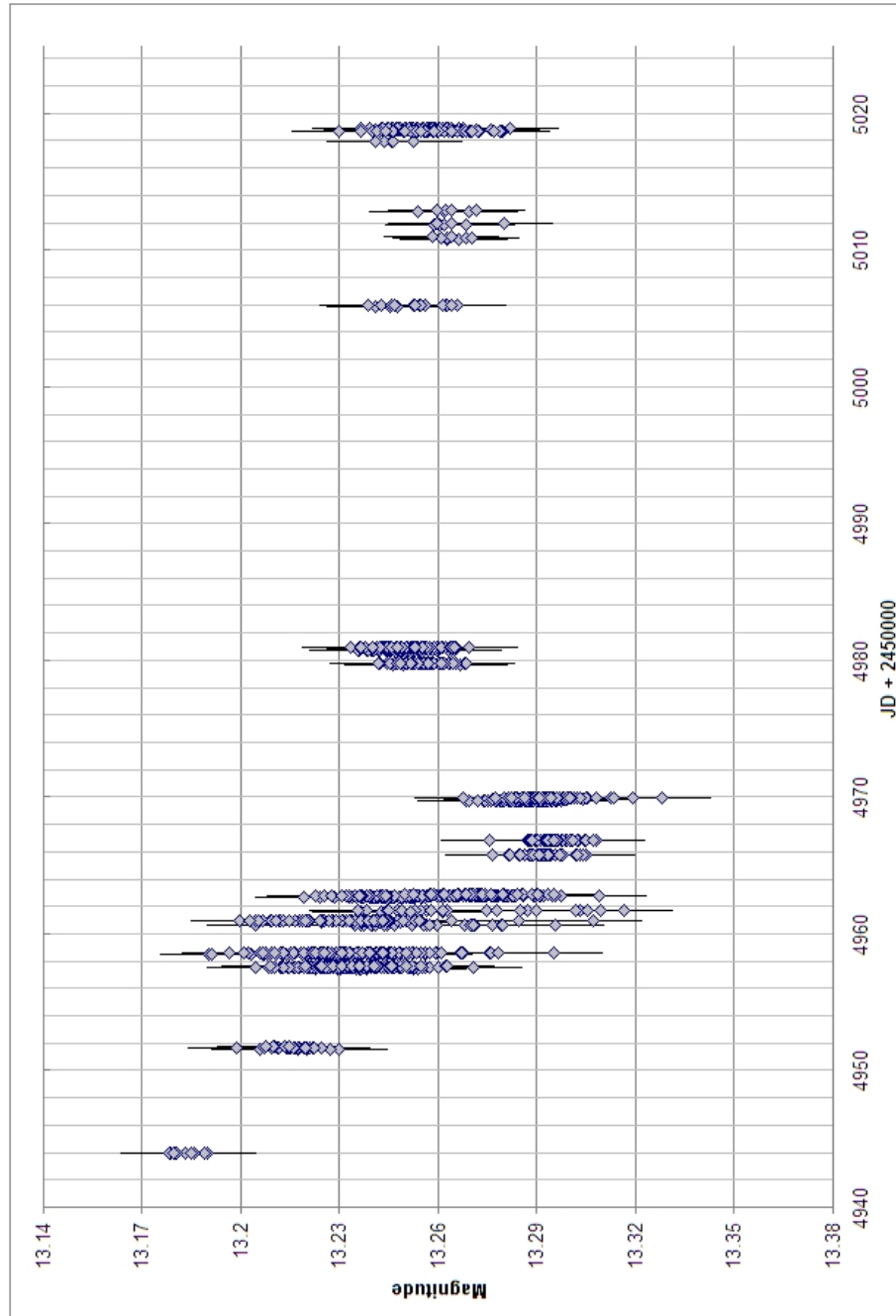
Figure 5.1 *R* band normal differential photometry from April 22 to July 6, 2009. These values are true apparent magnitudes of Mk501, adjusted from the six standard stars found in its FOV [15]. The error bars run ±0.02mag.
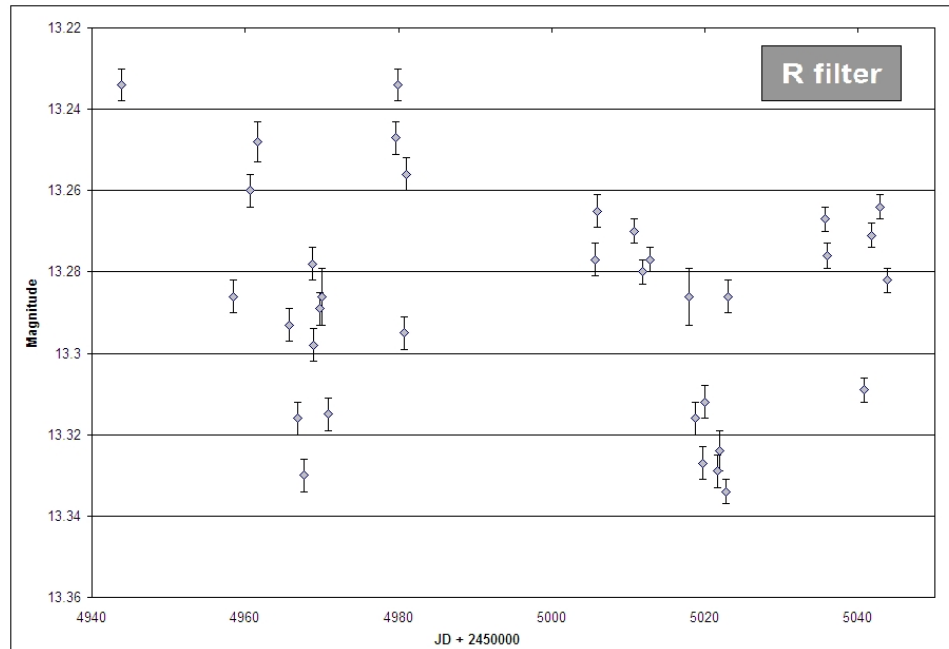
Figure 5.2 *R* band normal differential photometry from April 22 to July 31, 2009. These values were compiled by Alberto Sadun from the University of Denver, a collaborator. Each data point represents the differential magnitude of Mk501 from a five-image combined frame. Because these are not true apparent magnitudes, the error bars run at ±0.004mag.
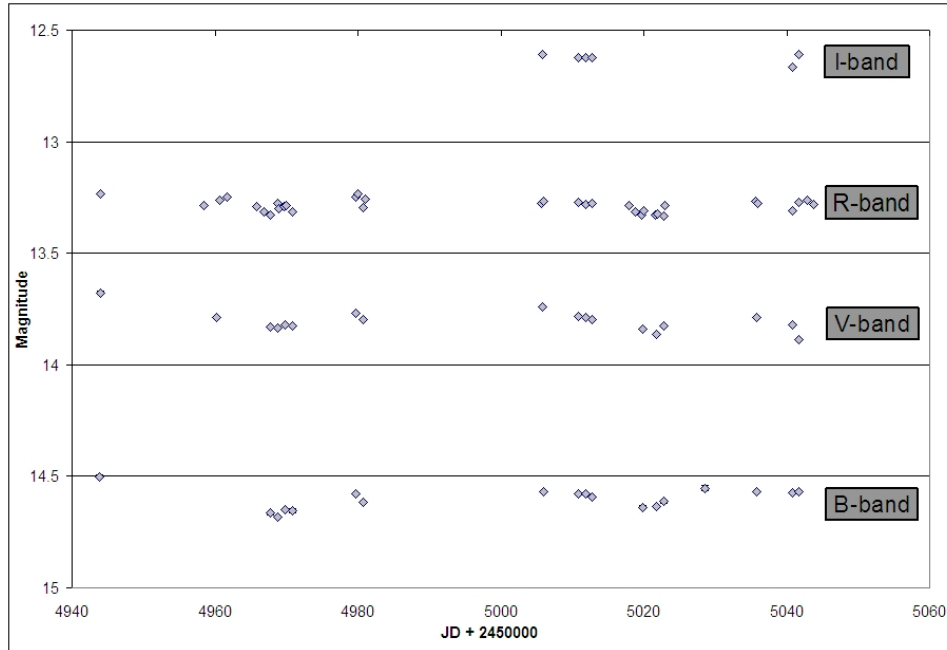
Figure 5.3 Normal differential photometry from Alberto Sadun for the B, V, R, and I bands. The R filter is shown exclusively in Figure 5.2, but it is shown here for reference and completeness.

objective questions and make reasonable conclusions.

As was mentioned in §3.3.2, our reductions of the Mk501 data turned from SBP photometry to normal differential photometry. But to prove the SBP photometry worked on brighter and bigger objects, we imaged another AGN—M81—which was previously studied with SBP photometry by McNeil [8]. Table 5.4 outlines his observations and findings. Discussion concerning the new ROVOR M81 data and McNeil's data are described in the following section.

5.2 Data Analysis

Multiple types of variations were searched for by the Mk501 campaign, as discussed in the introduction of this chapter. Therefore, this section will move through each type to discuss our findings; again they are IDV, intranight variations, and periodic

Filter	Image 1 Date	Image 2 Date	Day Separation	Variability (Δm)
B	11 Mar 2002	20 May 2002	70	0.057 ± 0.011
R	11 Mar 2002	20 May 2002	70	0.135 ± 0.011
B	23 Mar 1992	27 Jan 1995	1040	0.038 ± 0.011

Table 5.4 Differential magnitude variations obtained using surface brightness profile photometry. The two images dates are shown, as well as the number of days between the images, and their associated variation. Data retrieved from [8].

behavior. Reference to the Mk501 data will be in regards to the R band data, unless otherwise noted. Also, the data collected on M81 is discussed here.

5.2.1 IDV Data

Large amounts of R band images of Mk501 were collected on several nights. The high volume of images was to help look for IDV. Microvariability, or intraday variability, in Mk501 has been seen at timescales as short as 12 minutes, with a magnitude variation of 0.13mag [29]. A variation of 0.05mag was found over 15 minutes as well [28]. The goal of the ROVOR campaign was to further reduce the temporal resolution (timescales) of the IDV. The significance of finding IDV helps put limits on the size of the emitting region at the nucleus of Mk501[1]. Therefore, the smaller the temporal resolution, the more limited the model.

There have only been 3 nights that have displayed possible IDV activity. Those nights are 7 May, 11 May, and 6 July, 2009 and are shown in Figures 5.4, 5.5, and 5.6, respectively. Table 5.5 shows the information regarding the IDV associated with these nights.As can be seen, there is quite a lack of confident IDV values. The confidence

---

[1]Details regarding the derivation of this limitation is found in Appendix A.

parameter, $\mathfrak{C}$, is less than half of the 99% confidence value of 2.576. Visually, the IDV can be seen in the 6 May and 6 July data. We were not able to visually find IDV in the 11 May data and the $\mathfrak{C}$ value is not high either, but we had reason to believe—from previously processed data—that 11 May was more likely to have IDV. Instead, 11 May is a good example of the typical nightly data.

The scarcity of IDV in the Mk501 data highly suggests the quiescent state of Mk501. When Mk501 flares, IDV is highly active and has been consistently found. This ROVOR campaign hoped to find plentiful IDV values to help restrict AGN models. Sadly, as can be seen in Table 5.5, the Δm is generally on the order of its associated error and the $\mathfrak{C}$ values are low. These suggest the proposed IDV values are an artifact of the nightly seeing variations and not intrinsically from Mk501. However, if these values are real, a new lower limit has been temporally identified, with the $\Delta t = 8.59$min on 6 May. This places limits on the size of the emission region and extrapolates to the mass of the black hole region: 1.55×10^{11}m and 5.2×10^7 M$_\odot$. In fact, if the proposed IDV is inherent within Mk501, the designated R and M values fall within the range of currently accepted values of $0.01 - 3 \times 10^{11}$ M$_\odot$ [40–43].

Another intriguing note relates to the number of observations for each of these IDV nights. Each night included over 180 images. Therefore, it seems that the IDV is most likely to be present in nights with a large number of observations. This would mean that after further reductions, 11 more nights (with $N > 50$) are most likely to show IDV.

5.2.2 Intranight Variability

Intranight variability simply refers to how Mk501 varies from night-to-night. For this analysis, long-term monitoring was necessary. Figures 5.1, 5.2, and 5.3 show Mk501's magnitude from April to July 2009, spanning 100 days. When reductions

Date (UT)	N obs	Δm	Δt (min)	$\mathfrak{C}$	R (10^{11} m)	M (10^8 M$_\odot$)
07 May 2009	187	-0.019±0.009	8.59	0.996	1.55	0.52
11 May 2009	206			1.094		
06 July 2009	184	-0.01±0.01	38.87	1.244	6.99	2.37
06 July 2009	184	+0.01±0.01	19.53	1.244	3.51	1.19

Table 5.5 Display of the possible IDV nights, with the number of frames (N obs), the magnitude variation (Δm), the timescale of magnitude variation (Δt), the confidence parameter ($\mathfrak{C}$), the radius limit of the emitting region (R), and the mass limit of the central black hole (M). Notice that none of the days include a sufficiently large $\mathfrak{C}$ to be fairly confident in the Δm or Δt.
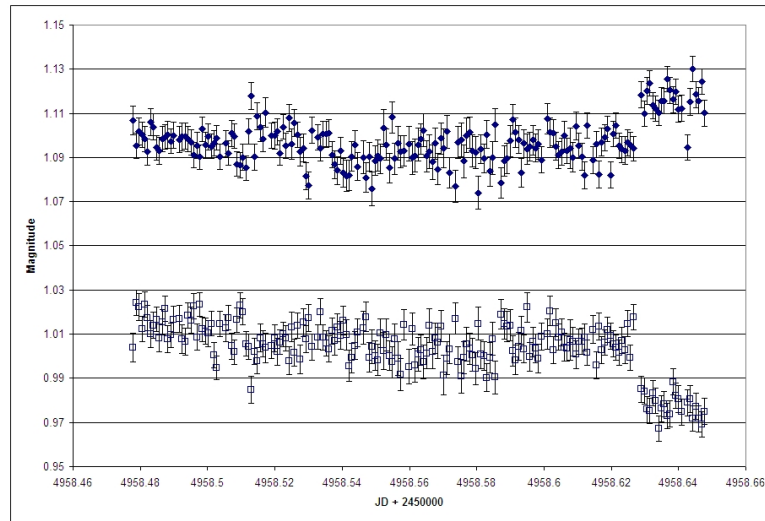
Figure 5.4 Normal differential photometry of Mk501 in the R filter from 07 May 2009. The Mk501 photometry (filled diamonds) was calibrated using star 1 as the comparison star and star 2 as the check star—see Figure 3.7. The differential magnitudes of the two stars are shown as empty squares. The stellar magnitude has been arbitrarily adjusted to fit on the same plot as the Mk501 differential magnitudes.
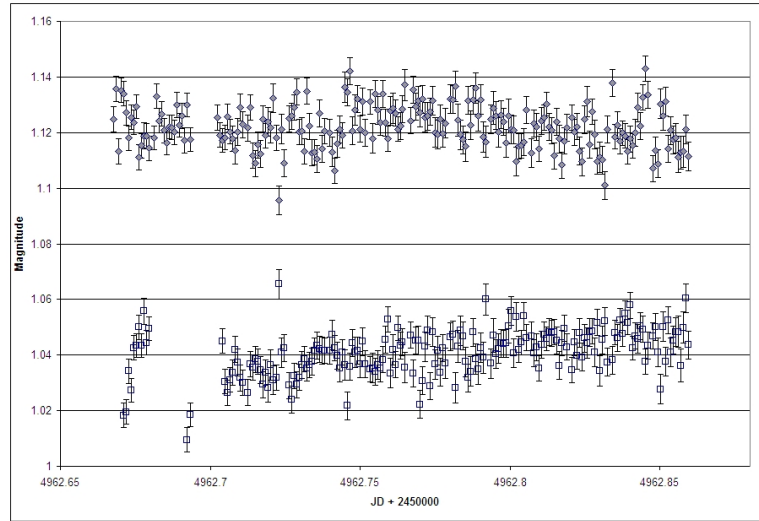
Figure 5.5 Normal differential photometry of Mk501 in the *R* filter from 11 May 2009. The Mk501 photometry (filled diamonds) was calibrated using star 1 as the comparison star and star 2 as the check star—see Figure 3.7. The differential magnitudes of the two stars are shown as empty squares. The stellar magnitude has been arbitrarily adjusted to fit on the same plot as the Mk501 differential magnitudes. This night represents a higher confidence value (§4.1.4) but no visible IDV.

and calibrations are completed, this campaign should span more than 330 days.

Analysis of the long-term data shows—again—the relatively quiescent state of Mk501. The *R* band only varies 0.1mag over the first 100 days. The maximum variation of 0.68mag occurred between 19 May and 28 May, or 8.776 days. This gives a change of about 0.08mag per day. The minimum variation was 0.003mag, occurring from 29 June to 30 June, or 0.999 days. This shows that between every night, significant variations occurred. Even though IDV may be mostly absent in a quiescent state, intranight variability is abundant. However, the relatively calm Mk501 leads the intranight variability to search specifically for low-amplitude periodic behavior.
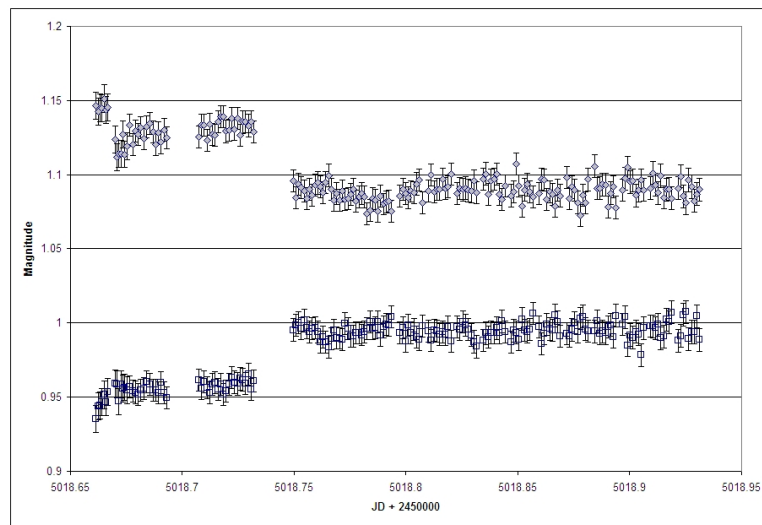
Figure 5.6 Normal differential photometry of Mk501 in the R filter from 06 July 2009. The Mk501 photometry (filled diamonds) was calibrated using star 1 as the comparison star and star 2 as the check star—see Figure 3.7. The differential magnitudes of the two stars are shown as empty squares. The stellar magnitude has been arbitrarily adjusted to fit on the same plot as the Mk501 differential magnitudes. Note the significant variation at the beginning of the night. This is an artifact of the flat fielding, as it is present in both the Mk501 and stellar differential magnitudes.

5.2.3 Periodic Variability

After establishing the prominent presence of intranight variability in Mk501's quiet state, searching for periodic behavior in that variability is the next step. As previously discussed in §4.1.4, no analytical computations were performed to identify periodic behavior. Visual analysis of the long-term plots was the basis of the periodic searches. However, no decisive results were obtained. It may be argued that a rough period of 20 days is present from the R band data in Figures 5.1 and 5.2. This would be consistent with a high-energy periodicity of 23 days found in Mk501 while in an active state [44]. But the difference between a quiescent and active state seems to be large, so a supposed relationship between these periodicities may be faulty. Additional reductions are required to portray the whole campaign; more solid periodicity measurements should arise.

5.2.4 M81 Data

The brighter, larger M81 galaxy was used to confirm the usefulness of the SBP photometry. As described in §3.3.2, Mk501 was just too small and too dim to provide adequate results with SBP photometry. McNeil was able to produce reliable variability values, as shown in Table 5.4 [8]. He found variations of 0.057 and 0.038mag in the B band, both with a ± 0.011 error. A $0.135 - 0.011$mag variation was found in the R band as well. Therefore, he showed SBP photometry was sufficiently accurate on M81.

We performed the SBP photometry on a couple of M81 images from 2 March 2010 to make certain this process actually works. After going through the SBP calculations, we conclude that the SBP photometry method does work. A differential magnitude of 0.005mag was found, with an associated error of ± 0.001mag. McNeil found larger

variations between images, but the two images used for the SBP photometry were separated by many days. The first set of images—the B and R bands—were 70 days apart; the third set was 1040 days. ROVOR's two 2 March 2010 images were only separated by 2 minutes. This shows the exciting power of the SBP photometry.

To further check the validity of the procedure, we performed the same final check that McNeil used [8]. After creating the SBPs for each frame and converting the magnitudes back into counts, the profiles are subtracted from one another. These values are then plotted versus the increasing radii. The resulting profile should be close to a Gaussian function with the same FWHM spread as the actual PSF of the image[2]; in fact, when proceeding with Images 12 and 13 from the 02 March 2010 ROVOR data, the final plot *is* a Gaussian and has a FWHM of 1.6 pixels (see Figure 5.7). The FWHM of the images was 1.95 pixels, creating a difference in FWHM values of 0.35 pixels. McNeil found a difference in FWHM for the M81 images of 0.5 pixels and claimed the "FWHM of the Gaussian profile *is* similar in size to the PSFs of the image" [8]. Therefore, the small variation of 0.005 ± 0.001mag is most likely intrinsically connected with M81.

---

[2]McNeil goes into further details about why this should be, but the simple answer is that the varying light (or remaining light) should be spread out the same amount as the rest of the frame [8]. A CCD's PSF is created by seeing and optics effects. Every point-source image should have the same PSF on the frame, including the varying jet in AGNs.
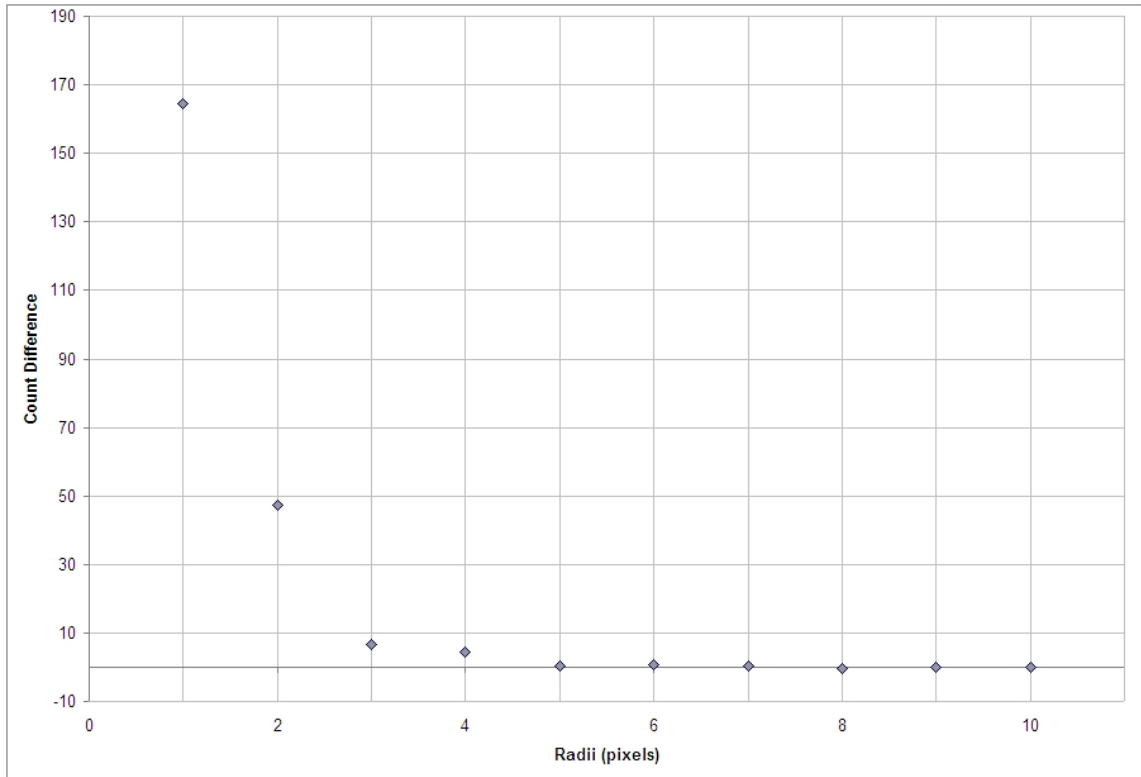
Figure 5.7 After the SBP photometry was completed on image 12 and 13 of M81 from 2 March 2010, the counts in each annulus $(\mathcal{C}_n)$ for each image is subtracted. Then, the resulting difference was plotted with the radius of the annuli on the x-axis, creating this plot. The FWHM of this Gaussian profile (1.6 pixels) equates with the FWHM of the PSF of the two images (1.95 pixels). Therefore, this plot establishes the credibility of SBP photometry on objects that are as bright and as large as M81.

Chapter 6

Conclusion

The year long campaign of Mk501 was generally successful. Possible IDV values of -0.019 ± 0.009, -0.01 ± 0.01, and 0.01 ± 0.01mag were found on rough timescales of 8, 39, and 20 minutes, respectively. The first IDV was found on 7 May 2009, with the last two coming on 6 July 2009. The calculated limitations on the radius of the emitting region and the mass of the associated blackhole lie within the accepted values for Mk501. This would lead one to think that the IDV is intrinsic. However, the size of the error associated with the IDV values and the low $\mathfrak{C}$ point to the IDV as a product of noise. Additional reductions and careful examination will reveal the true nature of the IDV.

Though intranight variability was identified every night for Mk501 from April to July 2009, periodic behavior was not satisfactorily detected. There seems to be evidence of a 20-day period, but the high error bars and relatively low amplitude intranight variability prevent this possibility from fully solidifying. Analytical programs—structure functions and `Period04`—were presented as a way to better identify periodic behavior in Mk501. These should be used to find periodic IDV and intranight variability in future data processing.

Additionally, after attempting to use the new SBP photometry technique on Mk501, we concluded that this particular blazar was just too dim and too small to produce viable data. This provided useful limitations concerning the SBP photometry reductions and permitted follow-up observations of M81 to compare with the McNeil (2004) data [8]. Between two, 2-minute subsequent images of M81, a differential magnitude of 0.005 ± 0.001mag was found. The FWHM of the residual light matched the FWHM of the image PSF within 0.35 pixels. This fits in the parameters of the SBP photometry and proves that SBP photometry should be used to identify low-amplitude variations, such as IDV.

Overall, the year long campaign will add a huge amount of data to the continuing observations of blazars and particularly Mk501. The data collected will be used to more fully constrain the present AGN models. Collaborations with other telescope facilities is highly recommended, especially to encourage simultaneous observations of Mk501 in the X-ray, γ-ray, or even radio regions of the electromagnetic spectrum. These simultaneous observations will show correlations between various regions and help solidify central blackhole theories.

The contents of this thesis were to guide students through the operation, reduction, and calibration processes associated with ROVOR and AGN research. This is, by no means, a complete collection of everything one would ever need to know concerning these topics. However, it was meant to simplify the learning process. A significant amount of time was used in coping with the nuts and bolts of a remote telescope facility and learning how to use the reduction tools in their most effective ways. This was to pass the knowledge on to others so that scientific progress can more readily move through BYU's Physics and Astronomy department.

Bibliography

[1] F. Cain, "How Many Galaxies in the Universe," (2009), Accessed April 2010.

[2] E. P. Hubble, "Extragalactic nebulae.," Astrophys. J. **64,** 321–369 (1926).

[3] O. D. A. Carroll, Bradley W., *An Introduction to Modern Astrophysics*, 2 ed. (Pearson Education, 2007).

[4] C. K. Seyfert, "Nuclear Emission in Spiral Nebulae.," Astrophys. J. **97,** 28–+ (1943).

[5] M. Ulrich, T. D. Kinman, C. R. Lynds, G. H. Rieke, and R. D. Ekers, "Nonthermal continuum radiation in three elliptical galaxies," Astrophys. J. **198,** 261–266 (1975).

[6] D. Gall and for the VERITAS Collaboration, "Multi-wavelength Observations of Markarian 501," ArXiv e-prints (2009).

[7] J. Quinn *et al.*, "Detection of Gamma Rays with E > 300 GeV from Markarian 501," Astrophys. J. **456,** L83+ (1996).

[8] S. R. McNeil, Ph.D. thesis, Brigham Young University, 2004.

[9] S. B. Howell, *Handbook of CCD Astronomy*, 2 ed. (Cambridge University Press, 2006).

[10] R. Ierusalimschy, L. Henrique de Figueiredo, and W. Celes, *Lua 5.1 Reference Manual*, http://www.lua.org/manual/5.1/manual.html, 2008.

[11] C. Pace, "BVRI comparison stars near selected very-high energy blazars," (2010), undergraduate senior thesis.

[12] A. U. Landolt, "UBVRI Photometric Standard Stars Around the Celestial Equator - Updates and Additions," **137,** 4186–4269 (2009).

[13] F. Murtagh, "Multiresolution Software Website," (2009), Accessed June 2009.

[14] A. U. Landolt, "UBVRI photometric standard stars in the magnitude range 11.5-16.0 around the celestial equator," Astron. J. **104,** 340–371 (1992).

[15] L. Heidelberg-Knigstuhl, "1652+398 (MRK 501)," http://www.lsw.uni-heidelberg.de/projects/extragalactic/charts/1652+398.html (Accessed April 2009).

[16] M. Villata, C. M. Raiteri, L. Lanteri, G. Sobrito, and M. Cavallone, "BVR photometry of comparison stars in selected blazar fields. I. Photometric sequences for 10 BL Lacertae objects," Astron. Astrophys. Suppl. Ser. **130,** 305–310 (1998).

[17] M. Fiorucci and G. Tosti, "VRI photometry of stars in the fields of 12 BL Lacertae objects.," Astron. Astrophys. Suppl. Ser. **116,** 403–407 (1996).

[18] J. R. Taylor, *An Introduction to Error Analysis*, 2 ed. (University Science Books, 1997).

[19] L. J. Walker, Helen M., *Statistical Inference* (Holt, Rinehart and Winston, 1953).

[20] M. R. H. Walpole, Ronald E., *Probability and Statistics for Engineers and Scientists*, 2 ed. (Macmillan Publishing Co., 1978).

[21] B. P. Roe, *Probability and Statistics in Experimental Physics*, 2 ed. (Springer-Verbig, 2001).

[22] L. Mortara and A. Fowler, "Evaluations of Charge-Coupled Device / CCD / Performance for Astronomical Use," In *Society of Photo-Optical Instrumentation Engineers (SPIE) Conference Series*, Society of Photo-Optical Instrumentation Engineers (SPIE) Conference Series **290,** 28–+ (1981).

[23] J. H. Simonetti, "Measuring the Signal-to-Noise Ratio S/N of the CCD Image of a Star or Nebula," http://www.phys.vt.edu/~jhs/phys3154/snr20040108.pdf (Accessed March 2010).

[24] M. V. Newberry, "Increasing Precision and Accuracy in Photometric Measurements," In *Precision CCD Photometry*, E. R. Craine, D. L. Crawford, & R. A. Tucker, ed., Astronomical Society of the Pacific Conference Series **189,** 74 (1999).

[25] J. Heidt and S. J. Wagner, "Statistics of optical intraday variability in a complete sample of radio-selected BL Lacertae objects.," Astron. Astrophys. 305 (1996).

[26] M. Jang and H. R. Miller, "The Microvariability of Selected Radio-Quiet and Radio-Loud QSOs.," Astron. J. **114,** 565–574 (1997).

[27] G. E. Romero, S. A. Cellone, and J. A. Combi, "Optical microvariability of southern AGNs," Astron. Astrophys. Suppl. Ser. **135,** 477–486 (1999).

[28] A. C. Gupta, J. H. Fan, J. M. Bai, and S. J. Wagner, "Optical Intra-Day Variability in Blazars," Astron. J. **135,** 1384–1394 (2008).

[29] K. K. Ghosh, B. D. Ramsey, A. C. Sadun, and S. Soundararajaperumal, "Optical Variability of Blazars," **127,** 11–26 (2000).

[30] K. K. Ghosh, C. Kim, B. D. Ramsey, and S. Soundararajaperumal, "Optical Microvariability of Blazars," Journal of Korean Astronomical Society **34,** 9–15 (2001).

[31] A. C. Gupta, W. G. Deng, U. C. Joshi, J. M. Bai, and M. G. Lee, "Multi-color optical variability of the TeV blazar Mrk 501 in the low-state," New Astronomy **13,** 375–384 (2008).

[32] A. A. Jensen, "Structure Function Analysis of Blazars AP Librae and 3c279," (2008), Undergraduate senior thesis, accessed March 2010.

[33] J. H. Simonetti, J. M. Cordes, and D. S. Heeschen, "Flicker of extragalactic radio sources at two frequencies," Astrophys. J. **296,** 46–59 (1985).

[34] P. Lenz and M. Breger, "Period04 User Guide," Communications in Asteroseismology **146,** 53–136 (2005).

[35] S. . NASA, "Hubble Essentials," (Accessed March 2010).

[36] R. D. Crisp, "Richard Crisp Homepage," (2009), Accessed September 2009.

[37] R. D. Crisp, in *Residual bulk image characterization and management in CCD image sensors*, E. Bodegom and V. Nguyen, eds., (SPIE, 2009), No. 1, p. 72490L.

[38] J. R. Janesick, *Scientific Charged-Coupled Devices*, 1 ed. (SPIE—The International Society for Optical Engineering, 2001).

[39] H. L. Johnson and W. W. Morgan, "Fundamental stellar photometry for standards of spectral type on the revised system of the Yerkes spectral atlas," Astrophys. J. **117,** 313–+ (1953).

[40] A. J. Barth, L. C. Ho, and W. L. W. Sargent, "The Black Hole Masses and Host Galaxies of BL Lac Objects," In *Active Galactic Nuclei: From Central Engine to Host Galaxy*, S. Collin, F. Combes, & I. Shlosman, ed., Astronomical Society of the Pacific Conference Series **290,** 601–+ (2003).

[41] J. H. Fan, G. Z. Xie, and R. Bacon, "The central black hole masses and Doppler factors of the gamma -ray loud blazars," **136,** 13–18 (1999).

[42] D. Merritt and L. Ferrarese, "The $M_\odot$-σ Relation for Supermassive Black Holes," Astrophys. J. **547,** 140–145 (2001).

[43] F. M. Rieger and K. Mannheim, "On the central black hole mass in Mkn 501," Astron. Astrophys. **397,** 121–125 (2003).

[44] F. M. Rieger and K. Mannheim, "Implications of a possible 23 day periodicity for binary black hole models in Mkn 501," Astron. Astrophys. **359,** 948–952 (2000).

Appendix A

Blackhole Radius and Mass Derivation

§5.2.1 describes a procedure that uses IDV data to place limits on a blackhole's emitting region and mass. The derivation of this limitation is included here. This is a useful calculation for checking the nature of the IDV. If there are already known values for the radius and mass of the blackhole, the calculated radius and mass should fit within those values. However, this does not mean that if a true IDV is found and does not fit within previously defined ranges that the IDV is actually faulty. Care must be used in determining and stating the nature of the IDV and subsequent radius and mass values.
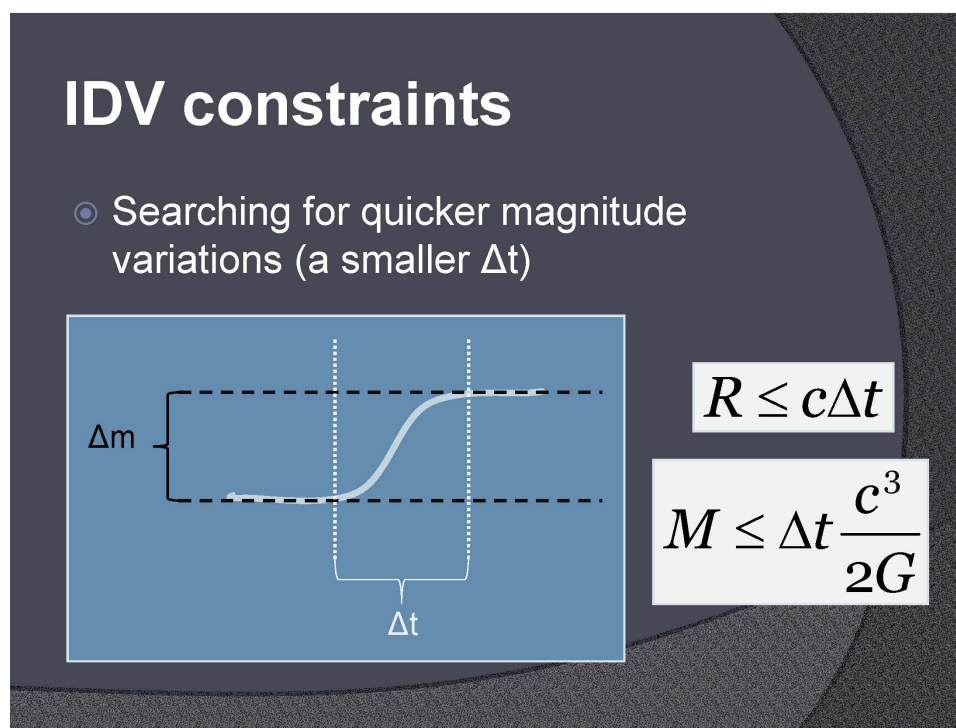
Figure A.1 This is a slide from a presentation I gave in April 2010. It shows a very basic example of what an IDV should look like in the data. Obviously, there is nothing that is going to be that smooth, but the idea of changing from one magnitude to another is easiest illustrated as such.

$$d_2 = \frac{(d_1 + R)}{\cos(\theta)}$$

take $\cos(\theta) \cong 1$, so that

$d_2 \cong d_1 + R$, or $d_2 - d_1 \cong R$;

$$\Delta t = \frac{(d_2 - d_1)}{c},$$

$$c \cdot \Delta t = d_2 - d_1 \cong R.$$

Including a relativity factor (due to higher redshift):

$$R \cong \frac{c \cdot \Delta t}{\gamma},$$

where $\gamma = \left(1 - \frac{v^2}{c^2}\right)^{-1}.$

Take $\gamma = 1$, then

$$R \leq c \cdot \Delta t.$$

Using the Schwarzschild radius definition, we can estimate the mass :

$$R_s = \frac{2GM}{c^2},$$

$$M = R_s \frac{c^2}{2G};$$

$$M \leq (c\Delta t) \frac{c^2}{2G} \text{ (where } R_s = R),$$

$$M \leq \Delta t \frac{c^3}{2G}.$$
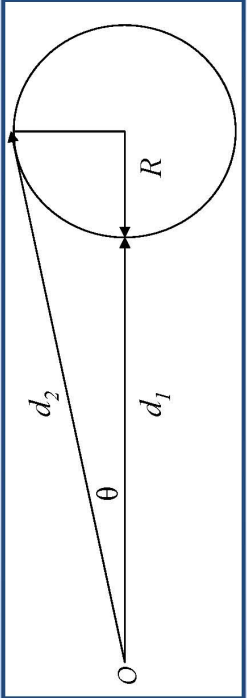
R = sphere radius

O = observer

$d_1 < d_2$

$R \ll d_1$

Figure and derivation adapted from *An Introduction to Modern Astrophysics*, Carroll, B.W. & Ostlie D.A. 2nd edition, 2007.

Figure A.2 This is the slide that followed the previous one. It goes through the derivation of the radius and mass limitations.

Appendix B

Troubleshooting with ROVOR

- If `Orchestrate` chokes through the night while following an object through the meridian, the problem is most likely that the object was within the meridian limits of the telescope. Those limits are displayed in `theSky` as a blue and red bang on either side of the meridian. A couple of things can be done to avoid or fix the problem:

  1. Plan the script to avoid any object within about 20 minutes of the meridian, on either side (that 20 minutes is actual time, not arcminutes). This is the easiest fix—just avoid the problem.

  2. `Orchestrate` can take a list of enumerated errors and disregards them if they occur in the script. You can search for details in the `Orchestrate` help file and on the Software Bisque website (www.bisque.com). Simply, there is a file with errors listed for `Orchestrate` to ignore. Using this shouldn't hurt ROVOR; it is fairly effective, too.

- If `CCDSoft` freezes during an image download (or if you accidentally aborted the download of an image), you can attempt a number of fixes in the following

order:

1. WAIT for a couple of minutes. The computer and/or CCD are confused, so just be a little patient.

2. Try closing `CCDSoft` and re-opening it. In doing this, you may have to reset the Autosave parameters again.

3. Try disconnecting from the CCD. Wait again to see if it responds.

4. If `CCDSoft` will not close or disconnect from the CCD, the last resort is to cut the power to the CCD. After this, you should be able to close `CCDSoft`; it may automatically close itself. Wait for a couple of seconds and turn the power back onto to the CCD. Then start up `CCDSoft`, reconnect to the CCD, begin cooling, and reconnect everything in `Orchestrate`. In fact, you may have to restart `Orchestrate` as well.

Just try not to abort any image downloads. Cutting the power to the CCD isn't a very fun thing to do.

- There have been a couple of times when everything has connected just fine— `CCDSoft` to the camera, filter wheel, and focuser; `theSky` to the telescope; `Orchestrate` to the telescope, the mount, the camera, and filter wheel—and yet, when you go to "home" the scope, it displays an error. The error it usually displays when it cannot find its home position is something to the effect of "Telescope could not be homed. Some telescopes do not support this command." This is probably true, but our telescope does support this command and it is essential to the telescope actually working after it has been parked.

It is most likely a mechanical problem. There is a tightening/locking screw

on the top part of the mount that permits the telescope to rotate but not slide from position. If that is too tight, it will not allow the telescope to rotate at all. We found this out when the temperature variations between day and night were large. At night (cooler), the mount would contract and the telescope would not be able to find "home". If `theSky` gives an error saying the scope could not find home, you must *manually* release the tightening screw: have fun driving down to Delta! When you get down there, the telescope *should* be beeping. That's its signal for not being able to move. If it is not beeping, however, there is probably something else going on (and I have no idea what that would be).

- If, for some reason, `Orchestrate` errors on a "Take Image" command, a number of sources of error are available:

  1. `Orchestrate` is not connected to the CCD.

  2. `CCDSoft` is not connected to the CCD.

  3. The arguments for the "Take Image" command were incorrect.

  4. `CCCSoft` froze during a download (see above).

  5. `CCDSoft` tried to save the file, but the disk space was full.

- Recently, we have had problems with incredibly slow internet connections. When logging into the computers down at the ROVOR site through the VNC connection, the screen reloads every ten minutes. After further investigations and a talk with HughesNet (the internet satellite provider), Bret Little was able to access an online service that records the amount of information downloaded per hour. For the record, we have a limited number of megabytes available to us each day. When that limit is exceeded, a very low downloading cap is placed on us by HughesNet. After looking at the amount downloaded per hour, we

noticed there was something downloading 30MB/hour. Then, the daily limit would be exceeded and the cap would be placed, thereby slowing down the VNC connection like crazy. There is a virus on the computer that needs to be removed. We replaced the computer and installed a virus scanner. Hopefully you don't have to go through those same issues.

Appendix C

ROVOR Weather Station

The actual program itself is quite a mystery and the places the text files are output are murder mysteries themselves. Therefore, here is the secret passageway to the text and ".exe" files:

$$\text{Weather}\backslash\text{WeatherStation}\backslash\text{sensor\_watcher}\backslash\text{debug}$$

To help cross all of this, a shortcut has been placed on the desktop of the computer to easily access the ".exe" file. The LabView program has the specific text file location embedded within it, also.[1] If this becomes a bit more tedious than it needs to be, contact Daniel Wilcox at the following email address: dwilcox.byu@gmail.com. Hopefully the weather station lives for a long time without needing repairs or upgrades.

---

[1]We have recently discovered that the ".exe" file needs to be compiled for each new computer that the weather station is going to be run. This requires Visual Basic or the Visual Basic C++ program. The Express Edition of these programs can be accessed on the Microsoft website. Once these programs are installed, follow the instructions found with the weather station to produce the application file. Once you do, the text files should be produced and a small black pop-up screen should output that the computer is talking with the weather station software. (When the black screen is not there, the weather station is not running.)

Still, the need to more easily dissect and present the current weather, weather trends, and past weather is a necessity. No steps have been taken in that regard, however. The physics department operates a weather station that sits atop the Eyring Science Center. It may be worthwhile to meet with the professor overseeing the station to discuss possible ways to analyze and provide an simple weather display of the features previously described.

Appendix D

Customized User Manuals

This includes customized user manuals for setting up, running, and operating the
ROVOR telescope. These were compiled by Cameron Pace (the TPoint model and Or-
chestrate instructions) and Richard Pearson (the installation instructions). There are
so many intricate pieces to the ROVOR facility that not all of them were included in
these manuals, but hopefully they provide some quality assistance. If additional help
and assistance is needed, Richard can be reached at rlpearson_the_third@yahoo.com.

There is an account on gmail for ROVOR:

rovor.byu@gmail.com**, password: outhouse -- there is chatting capabilities on the left-hand side**

Installation Anew

1. Insert Paramount CD. Click on the "Install Software" button.
2. Install MKS 4000 USB Driver.
3. Install CCDSoft Software. Serial Number for CCDSoft should be written on an email to Dr. Moody. It should just be in the front of the CD case. If not, here it is for Physics and Astronomy Department / Brigham Young University: D068-9F6160FF. If CCDSoft cannot find the SBIG Driver and if it does not ask you to download the .cll files, then go to CCDSoft when it is uploaded and have it open the SBIG Driver Checker. (If CCDSoft cannot find the SBIG Driver and if it does not ask you to download the .dll files, then go to C>ProgramFiles>SoftwareBisque>CCDSoft> CameraDrivers>SBIG when it is uploaded and have it open the SBIG Driver Checker. Download and then Update. Now, this is only if you need the SBIG .dll files.)
4. Install TPoint Software. The Serial Number for Tpoint is written on the CD (brilliant, whoever did that (me)!); just in case, for Physics and Astronomy Department / Brigham Young University:
   1066-FE266053.
5. Install Orchestrate.
6. Eject the Paramount CD. Insert TheSky6 DVD (it should be just one DVD—there are 4 CD's if you wish to go that route). Again, the serial number should be written on one of TheSky6 CD's; Disc #2, I believe. If you can't find it, here it is:
   5050-C6396046.
7. Eject TheSky6 DVD. Insert the Paramount CD back in and install TheSky6 Update Driver.
8. You will notice that there are two functions that we do not use: IAClient and IAServer. These are used if there are going to be other people at different locations using ROVOR. If at some point you find that they would be helpful, they're here and waiting.
9. You will also notice that there is an "Optional Software" button, with features that include PrecisionPEC, Automapper, and TheSky Pocket Edition. The latter is not needed at all for ROVOR. We looked into using AutoMapper, but found that it was more of a problem than it was worth. So just use the directions on how to map and run a TPoint Model that we have put together. It is actually quite simple. PrecisionPEC would be useful if we were to get a Guider put on ROVOR at any time. It costs somewhere around $100, but again, it would not be helpful unless ROVOR had the ability to AutoGuide.
10. Next thing to do is to check for updates for each of these products. To do this, you have to go to the Software Bisque website, www.bisque.com. On the left side you'll see "Support Center." Click it. Then on the subsequent screen, click "Free Updates" on the right side. Sadly, you have to actually go to the site every time to get the updates, and they actually come relatively frequently. So check often. If they require you to sign in to their site, use this to sign in (unless you want to create an account for yourself): USER NAME> rlpearson, PASSWORD> outhouse. You can then go to "Downloads" and "Download Free Updates".

11. Find TheSky6, CCDSoft, Orchestrate, and TPoint Updates for Windows. Download and install them from the Desktop.
12. As of March 7, 2009, the versions should be:
    a. TheSky6   6.0.0.61
    b. CCDSoft   5.00.092
    c. Orchestrate   1.00.035
    d. TPoint   1.00.511
13. One more download place to check: Download Hot Fixes. Sometimes they put random, IMPORTANT things in here. Check every so often.
14. There are still more things to download. Go to www.rcopticalsystems.com to get the firmware for the TCCII that is attached to the telescope. Go to Accessories>Telescope Command Center. Then click on the link to the Software / Firmware. Find the Full Installation Package. Download it. Then go back and update the Firmware as needed.
15. Still, more things to download. Go to the Finger Lakes Instrumentation website, http://www.flicamera.com/index.html to get the driver for the filter wheel. Go to Support>Software. Download the FLISetup package.
16. Now we need to make sure that a configuration file is located in CCDSoft for the CCD that is being used. Currently, we are using an AP47p. Hopefully it is in the Configuration File in CCDSoft. If it is not, then we should have the driver around. Also, CCDSoft will need the INI file for the camera. We should have all those too. It is a file Folder called "Apogee". It can go into the Configuration File in CCDSoft as well.

MIRA Installation

1. We are using this program given to us by Michael Newberry, one of Dr. Moody's friends. He is very helpful and very open in suggestions. We have the 7th edition, but there is now a newer version. If you can convince Dr. Moody to get the newer version, then all of this is for naught. But until he does, this is the thing to use to upload the program.

2. There were a number of issues with the first couple of 7th editions. Finally, Mr. Newberry sent us the final "fixed" version of the 7th edition in the rovor.byu@gmail.com email.

3. You can either search "MIRA" on the email, or go to December 28, 2009 and look for the email from support@mirametrics.com. There is a pdf file that you need to download in order to upload the mira.exe file from the Mira FTP site. Also included in that email is a password to open the pdf. It is also given below:

Cu:wiwuipo44

4. Input the password and open the pdf.

5. Under the "Downloading MIRA Pro Ultimate Edition" section, go to the FTP site, download and install the Mira program. You will need to rid the computer of any other editions on the computer. The given passcode to install is given in the pdf or below:

66375-c43-aahf3-677-ffgh-ccxk-94kku

6. Once it's downloaded and installed, that should be it; though, you might need the code above to install it.

Orchestrate Setup

1. Once Orchestrate is open, go to View>Properties>Client. This will allow Orchestrate to connect to TheSky, CCDSoft, the Telescope, and Filter Wheel. You must find the name of the machine that is being used. This is found under System Properties>Computer Name. The "Full Computer Name" is what you will put in the Machine Name in Orchestrate. Then put in the user name and password of the machine you are using (the login you used when the computer starts up). In the case here, we use ROVOR-02 for the Machine Name, "rovor" and "outhouse".
2. For filters, instead of using names, we use numbers. Here are the numbers associated with each of the filters:
   a. 1 = Hα Narrow
   b. 2 = Hα Wide
   c. 3 = B
   d. 4 = V
   e. 5 = R
   f. 6 = I

Filter Wheel Setup

1. Once you have downloaded and installed the FLISetup package for Windows from the Finger Lakes Instrumentation website, you need to make sure that the USB connection for the filter wheel is in place. When it is, and the computer recognizes that it is there, then continue.
2. On the Start menu, go to All Programs>Finger Lakes Instrumentation>FLI Filter. This is actually the only program that we will end up using for ROVOR, so if you deem it necessary, the other programs can be removed as well.
3. When you first open FLI Filter, it will ask you to designate a port for the software to speak to the filter wheel. Select the option to have it scan for the USB connection (and if you wanted, have it search the serial ports too, just for fun) then click "Scan." It should find a port that it labels "flifil1." Click "OK."
4. Then, you will see a screen with a list of six slots, from 0 to 5. In the bottom corner is a message that reads its current position. It will say "Unknown." Click "Home." Wait for the message to show that it has actually found what filter it is at. You are then ready to change the filters.
5. PROBLEMS: If you have done all the necessary things above and FLI Filter still won't connect or if CCDSoft won't connect, then there are a couple of things to make sure of.
6. CCDSoft Troubles: The main problem here is that there are a couple of files missing that CCDSoft needs. In Program Files>Software Bisque>CCDSoft>Filter Wheel Plug Ins, CCDSoft needs the Finger Lakes Filter Wheel PlugIn.dll (1.0.0.6). That same file needs to be in CCDSoft>Filter Wheels>Finger Lakes. One last, very important thing: in C:/>Program Files>Common Files>System. There is a .dll file there that CCDSoft needs. It is called 'libfli.dll'. If you right-click on it, you will see that this was created around September 25, 2006. This one needs to be updated. So, back in C:/>Program Files> Finger Lakes Instrumentation, you will find the same

file, 'libfli.dll', but if you right-click it, you will see that it has been update and has a new date of around July 24, 2008 (or something newer). Copy that one and paste it into the Common Files, replacing the older one.

How to make a TPoint model

This article is intended to help you understand the process of creating a TPoint model. It is *not* intended to substitute diligent study of the TPoint manual and other resources. This article will touch on collecting data points, controlling the telescope and the camera using TheSky6 and CCDSoft, using Orchestrate to set up an automated mapping run, choosing which terms to use with the TPoint model, and other subjects.

- **What is a TPoint model?**

A TPoint model is a model that accounts for the inherent mechanical errors of a telescope that affect the telescope's ability to point directly at its intended target. With this model in place, TheSky6 can give the telescope "modified" directions so it will point more closely to its intended target. As expected, a good TPoint model requires a thorough understanding of the intrinsic errors of the telescope. This understanding only comes by pointing at many, many stars and recording the results. The TPoint model can only account for the periodic or repeatable errors of the telescope. Some errors, like those caused by mirror flop, are very difficult to address and cannot be corrected using TPoint. TPoint has many formulae or algorithms each designed to correct for a specific type of pointing error. The most challenging part of creating a TPoint model is deciding which of these algorithms or "terms" to include. The process of choosing terms is as close to an art as TPoint will ever get. As much time can easily be spent mulling over which terms to include as can be spent collecting the data points. There are many ways to simplify the process of including terms which will be discussed later.

- **What are data points?**

A TPoint model is made up of several data points. These points are used to map out and account for the pointing errors of the telescope. For example, suppose you point the telescope at Sirius which is located at 06h 45m 30.79s, -16º 43' 32.452". Because of errors in the worm gears, the telescope not having an exact polar alignment, flexure of the telescope tube, and many other things, the telescope will not point exactly at Sirius. It will point somewhere close to Sirius, say 06h 45m 33.5s and -16º 43' 36.54". When you tell TPoint to "Map" this data point, TPoint will note the RA and dec of the target object, the RA and dec of where the telescope actually pointed, and the angular separation (known as the pointing error) of the two. With a large collection (100-200 points) of this data in hand, TPoint can account for many of the errors which caused the scope to miss its target and pointing will greatly improve.

- **How often does a new TPoint model need to be made?**

Anytime changes are made to the telescope, such as when the polar alignment is adjusted or a new camera or filter wheel is installed, a new model must be created. You might be able to get away with doing a "Short Mapping Run" as described on pages 31-33 of the TPoint manual. With a short mapping run, some of the terms are adjusted, but not all of them. If this doesn't work, you will have to start over and make an entirely new model. This isn't that big of a deal if you are using the automated method described below.

- **Collecting Data Points**

The process of collecting data points is referred to as "mapping". There are two *very* different ways of mapping these data points. The first method requires more direct input from the observer; the second method is almost entirely automated. You should have some practice with and a good understanding of the first method before you attempt the second. Before doing a mapping run, it is important to decide where in the sky the points will be taken.

First, TPoint will not work with less than 6 points. Once you have mapped six points, TPoint can start improving the scope's pointing. Because of this, you won't be able to use the second method listed above to map these first six points. Also, these first few data points will exhibit large errors. You may even have to have someone stand on a ladder and look through the finder scope to give you directions as you use the motion controls in TheSky6 to center the scope on the desired star. Another thing that will help while mapping these first few stars is to map a group of stars that are bright and close together. If the stars are bright enough, you can even map them before it is fully dark. The bright stars in Leo or Orion are good examples of stars to use for these first six data points. These first six stars **must** be on the same side and ideally the **west side** of the meridian when you map them. If you have your heart set on mapping Orion and some of Orion's stars are east of the meridian and some are west, TPoint will have a meltdown. Splitting up the first six stars like this is disastrous and you will have to start over.

After you get these first six down, there are a few decisions you have to make. You will have to decide how many points to map, how far down in altitude you want to go, and which method to use. Before we discuss these decisions in any more detail, let's get a good look at the first method of mapping.

- ○ Method 1
(Quick start: just follow the items in italics to start mapping stars right away.)
The first method is just as described above: pointing the telescope at a star and recording the error. This is accomplished in 7 or so steps.

1. Insert a TPoint object into TheSky6.
2. Choose a star.
3. Use TheSky6 to tell the scope to slew to the selected star.
4. Use CCDSoft to take an exposure of the star.
5. Based on the exposure, make slight adjustments to the scope.
6. Take exposures and make adjustments until the star is centered.
7. When the star is centered, tell TheSky6 to "map" the star.

This method requires a lot of user input, is very time consuming, and may be a bit frustrating. Keep in mind though that it is important to know how to do it this way. This is just like long division; you know how to do it so you can still divide when you don't have a calculator. When large pointing errors appear, such as when mapping the first

six points or crossing over the meridian, this technique may be the only way to go. The automapping feature of method two cannot handle very large errors and when it fails, you will have to do it manually as described above. Let's look at each of the above listed steps in detail.

1. Insert a TPoint object into TheSky6.
(From TheSky6, click **Edit | Insert New Object… | TPoint Model** *then click ok).*
You have to insert a TPoint Model object into TheSky6. This allows TheSky6 to enter the mapping data into TPoint.

2. Choosing a star.
(If you have never mapped a star before, don't worry about the following stuff. Just pick a bright star and get started with the next step.)
As mentioned above, you have some decisions to make after mapping the first six stars. First, it is a good idea to map a bunch of stars on the west side of the meridian before hopping over to the east side. There are a couple of reasons for this. If you flip over to the other side of the meridian too early, TPoint will have trouble modeling your data points. Richard and I did this once and the pointing error kept getting bigger and bigger. There was no hope of salvaging (or even understanding) the model, so we had to start over after two or three hours of work. Map at least 20-30 points on the west side before starting to map the east side. Also, looking at stars on the opposite side of the meridian requires the scope and counterweight shaft to switch places. This takes a couple of minutes to do. The more times you flip from one side of the meridian to the other, the less time you will have for mapping. If you drove down to the ROVOR site to do the mapping run and you are using this method, every minute will be precious and you won't want to waste time.

Another decision you will have to make is how far down in altitude you will go. The mirror of the ROVOR scope is fixed, so it won't roll out and shatter on the floor. In other words, the telescope itself can be safely pointed at objects that are right on the horizon. In practice, you will never observe objects that are close to the horizon. Suppose you want to observe an object that is currently at 30⁰ altitude. If your TPoint model included stars that were at about that same altitude, the scope will have a hard time tracking the object you are observing. It is a good idea to map stars that are at a lower altitude as part of your model. If you want to observe at 30⁰ altitude, it would be a good idea to map stars down to 20⁰ altitude. Mapping stars close to the horizon is difficult because refraction starts causing problems.

As was mentioned earlier, this method works best with bright stars. The TPoint manual suggests using stars of sixth magnitude or brighter. The reason for this is to avoid confusion: the greater proportion of dimmer stars makes it easier to confuse them. This is one of the drawbacks of this method. Because there are only so many bright stars, it would be hard to get a model with a huge number of data points. As the stars march westward over the course of the night, you can map the same stars over and over again because their altitude and azimuth have changed.

As you add points to your model, a little numbered red line appears on TheSky6. This line is like the crumbs that Hansel and Gretel left behind them to find their way out of the forest. This red line will help you visualize where you have mapped and where you have not. You can read more about this line on pp. 24-25 of the TPoint manual.

3. Slewing the scope.

BE CAREFUL

DO NOT SLEW
THE TELESCOPE
WHEN THE DOME
IS CLOSED
OR ONLY PARTIALLY
OPENED.

(Click on the star in TheSky6. This brings up the Object Information dialogue box. Along the bottom right hand side of this box is an icon of a little green telescope. Click on this icon. You will be asked to confirm the slew. Click ok to confirm. The telescope should start slewing.)

Before you can use TheSky6 to tell the scope where to point, there are a few things you need to make sure of. First, make sure TheSky6 is connected to the telescope. To do this, click on **Telescope | Link**. This should establish a link between the scope and TheSky6. If it doesn't, check the troubleshooting section.

Once TheSky6 is connected to the telescope, you are ready to give the scope some orders. Click on the star you want the scope to point at; this brings up the Object Information dialogue box. Click the **slew** button: it is the icon in the lower right corner of the box that looks like a little green telescope with a red arrow by it. This will make the scope point at the currently selected object. Be sure the object listed at the top of the box is indeed the target you want to point at.

You will be asked to confirm the slew. Click ok and the white crosshairs indicating where the scope is pointing should start moving toward the target. Of course, the telescope should start moving as well (be sure that nothing is in the way of the scope as it slews). Wait for a few seconds after the white crosshairs settle on the target so you don't accidentally take an exposure while the scope is still moving.
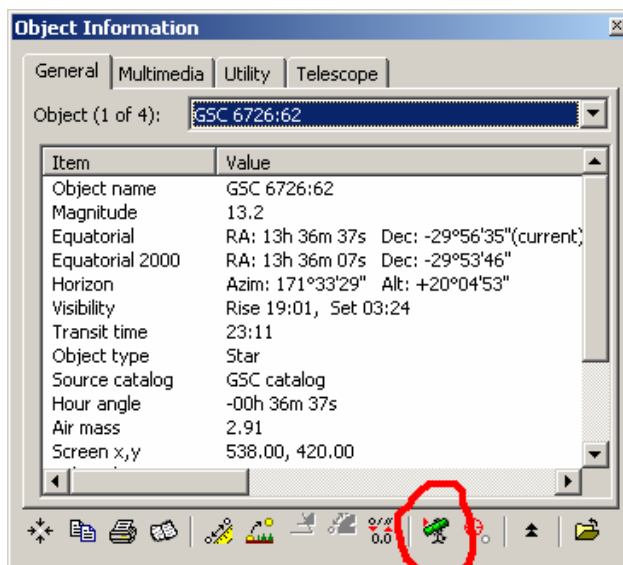
This is the Slew Button

4. Use CCDSoft to take an exposure of the star.
*(Go into CCDSoft. In the **Take Image** tab of the Camera Control dialogue box, set **Bin** to **2x2**. In the **Exposure** portion of the box, be sure **Minutes** is set to **0**, and set an appropriate number of **seconds**, maybe **1** or **2**. Now click the **Take Image** button to take a picture.)*
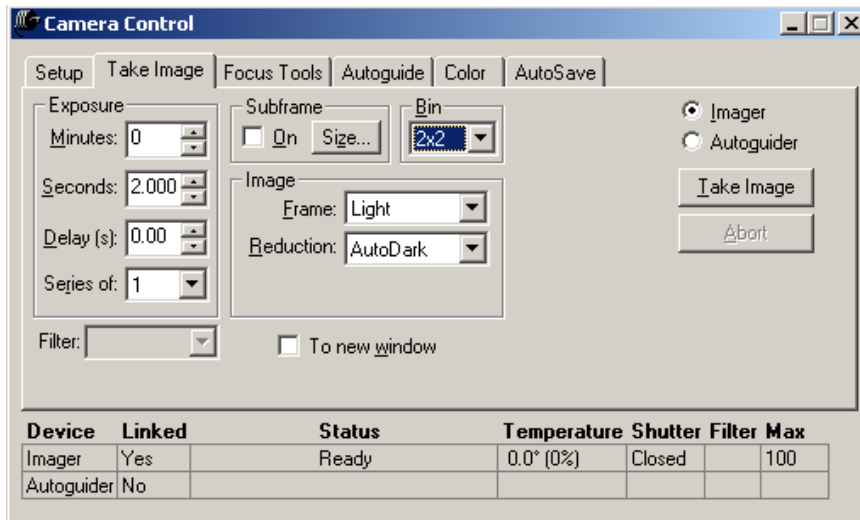
It really isn't that hard to take an image. Just be sure you have the correct exposure time entered in. Also, be sure CCDSoft is connected to the camera. These exposures we are taking for mapping purposes don't have to be professional quality or anything. You will have to play around with the exposure time to get it right. Sometimes you need a couple seconds, other times a tenth of a second is enough. You should definitely set the **Bin** to **2x2**. This will lower the resolution, but for these pictures you don't care about that. Binning 2x2 will make the download time a lot faster. This method is already time consuming, and you will want to cut every corner you can. When you click the **Take Image** button, you should hear a soft click as the camera shutter opens. As the exposure is being taken, the **Status** bar will slowly fill with blue, indicating the elapsed time of the exposure. At the end of the exposure, you will hear another click as the camera shutter closes. In other situations, you will need to pay close attention to when the shutter opens and closes. At the end of the exposure, the CCD will start to download the image to the computer. Depending on how you set the Bin, this downloading process can take anywhere from fifteen seconds to a minute and a half. The scary thing about downloading is that the computer screen freezes while the image is being downloaded. You can't move the mouse or get any sort of response out of the computer. **Don't worry**. This is part of the process. Just be patient and in a little while the computer will return to normal and you will have your picture.

You can use the following trick to save time by starting taking exposures before it is even dark yet. Since TheSky6 knows the coordinates of all the stars, you can point the telescope and start taking images before you can even see the stars with your naked eyes. For example in April-May, Leo is just above the sun and has many bright stars to use for your TPoint model. After the sun has gone down but it is still not quite dark enough to see the stars, try using TheSky6 to point the scope at Regulus and take a short (.10 second) exposure (Be **very very** sure you know what you are doing). Because the CCD is much more sensitive than your eye, you can usually get a picture of Regulus (or any other bright star) this way. You can use this technique to map data

points before it is even dark enough to observe yet. This way you can spend more time working instead of standing around with your teeth in your mouth waiting for it to get dark.

     5. Based on the exposure, make slight adjustments to the scope.
(In CCDSoft, hit the 6 key to get the crosshairs to appear. Use the Motion Controls to center the image in the crosshairs. This will take several iterations.)

After you have taken an exposure, you now need to make slight corrections so your target star will be in the center of the image. Hit the 6 key to get the crosshairs to appear. Without the crosshairs, it is very hard to get the image centered.
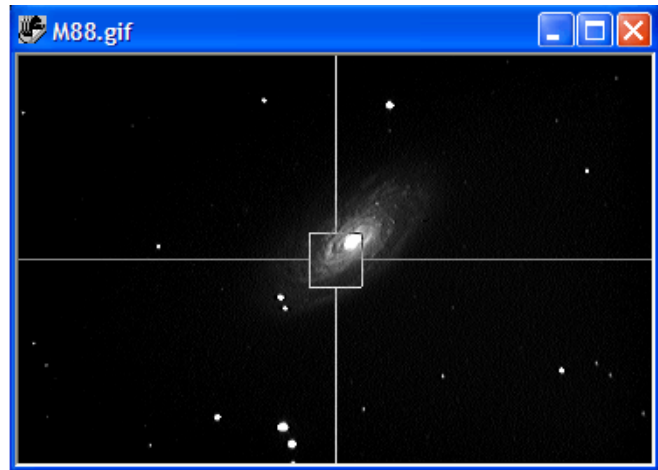
So, lets say the star you just took a picture of is slightly above the center of the image. Now you need to decide what corrections to make to get the star in the center. It will not be obvious what direction you need to move the scope to get the star centered. You will just have to pick a direction, slew the scope that way a little bit, take another exposure, and see what the results are. The first few stars of the night will be a challenge because you don't know yet how the directions on the Motion Controls correspond to the directions on the exposure. In our experience, the axes of the motion controls are flipped in relation to the axes of the exposure when you take exposures on the other side of the meridian.

I have been talking a lot about the Motion Controls. Let me explain what they are and how to use them. The motion controls are a little dialogue box in TheSky6 that you can use to direct the motion of the scope. They are like the electronic counterpart to the hand paddle motion controls. Instead of the joystick you click on the button of the direction you want to go. You can read more about how to use the motion controls on page 231 of TheSky6 user guide. Click on **Telescope | Motion Controls** to bring up

the controls. You can change the controls to move in Ra and Dec or in Alt Azm. You will want to leave them in Alt Az. In the picture on the left you can see there is a little radio button that says "Move," but it is grayed out. When you bring up the motion controls on the computer connected to the ROVOR scope, this button will not be grayed out. Be sure to select "Move" rather than "Jog." You can set the rate of motion relative to the sidereal rate. 16x is ok for big moves, but for fine tuning use 4x or even 2x. As was mentioned above, for the first picture you will just have to pick a direction and go with it. Hold down the button you chose and the scope will move a little bit in that direction. You should hear the servos in the mount move as the scope slews.

6. Take exposures and make adjustments until the star is centered.

Once you think you have moved the scope enough, go back into CCDSoft and take another exposure. You should be able to tell from the new exposure if you guessed the right direction. If you guessed wrong, try moving along the other axis. If you moved too far, you should change the "Move" setting in the Motion Controls to a lower slew rate. If the star seems so big that it fills the center of the crosshairs, you may need to set the exposure to a lower time. If the star is bright and you have a long exposure time, it will just be a big blob of light. To do this right you will want the star to look more like a point.

After a few iterations of taking exposures and making adjustments, you should get the star pretty close to the center of the crosshairs. As you get it close enough that you only have to make slight adjustments, you should set the Motion Controls to slew at 2x. After you figure out how the N S E W buttons on the motion controls correspond to the axes of the exposure, it will be easier to fine tune the motion of the scope.

7. When the star is centered, tell TheSky6 to "Map" the star.
*(Click on the **Map** button by the slew button on the Object Information dialogue box to map the star. If the star seems way off, you will be prompted to confirm the map. Click ok to confirm.)*
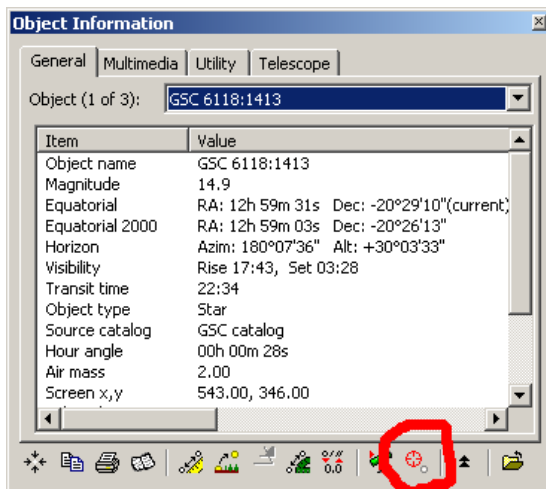
This is the Map button

This is easy. Just click on the **Map** button by the **Slew** button. If the star seems way off, you will be asked to confirm the map. Just confirm it.It will take some time to master this process, but it is something you have to know how to do. As you map more and more stars, the pointing will improve and you won't have to make so many adjustments to get the star centered. Once you have thirty or more stars, the TPoint model will have enough data to support more terms.

- **Selecting Terms**
  (Add terms that will improve the RMS pointing of the model)

Now that you have a statistically significant sample, you can begin adding terms for TPoint to account for. There are six basic terms that TPoint starts out with. You can read up on what these terms deal with starting on page 42 of the TPoint manual. I will not explain them here except to say they account for non-perpendicularities in the telescope mount and the polar alignment being off. As was mentioned at the beginning

of this article, TPoint can account for many other things. These other terms are what really help TPoint adjust the pointing of the ROVOR scope.

Before we talk any more about selecting terms, we need to talk about some vocabulary words. Selecting terms for the TPoint model requires a decent understanding of statistics. Rather, it requires a decent understanding of a few statistics words.

Root Mean Squared (RMS) –The RMS basically tells you how well the scope will point at something. For example, if the RMS is 40 arcseconds, that means the scope will usually point to within 40 arcseconds of your intended target. You will want the smallest RMS possible, ideally less than 30 arcseconds.

Value – This is a measure of how important a given term is to the TPoint model. The higher the value, the more that particular term is contributing to the model. A term with a small value or a value that is smaller than its sigma should not be used. Ideally, all terms you use should have a value that is at least three times greater than the sigma.

Sigma – This is the measure of the error of individual terms. A term with a large sigma has a large standard deviation. That means TPoint can't really tell if this term is helping the model at all. Do not include terms with a large sigma, even if they improve the RMS.

Population Standard Deviation (PSD) – This is a measure of the Sigma of the whole group of terms. You want keep this value as small as possible.

The basic idea of making a TPoint model is to statistically improve the pointing of the telescope. Your task in creating a TPoint model is to minimize the RMS. The terms you add will account for different mechanical problems within the scope and improve the RMS. You must be careful, however, not to increase the PSD. The point is, if you add a term that makes the RMS go down but increases the PSD, that term did more harm than good and you should not include it. In the end you want the lowest RMS possible without increasing the PSD.

There are two different approaches to making a TPoint model. We will try to chart a middle course between these two approaches. First, terms can be added that will account for known problems with the scope. For example, the telescope tube will almost certainly flex as you slew around the sky. You will want to use the TF-Tube Flexure and/or the TX-Tube Flexure (tan) terms to account for the tube flexing. As you become more familiar with the ROVOR scope, you will notice other specific errors to account for. This first approach centers around the idea of having a well-understood model that accounts for well-understood problems. The other approach is to make a model and add terms that make it work better without necessarily understanding the specific problems the terms are accounting for. This second method could be said to be the "Empirical Evidence Approach." The best thing to do is to use the terms that prove to be statistically significant (have a large value) and then see if any "Empirical" terms can be added to clean it up a little.

After you have your data set, the following sequence will almost always result in a decent model. First, right-click on the TPoint Model object in the upper left corner of TheSky6, then go to **TPoint Model Object |Open** to open TPoint. You will see an Excel spreadsheet type layout. To edit the terms that are being used in your model, click on **Model| Fit Data…** This will bring up the following window.
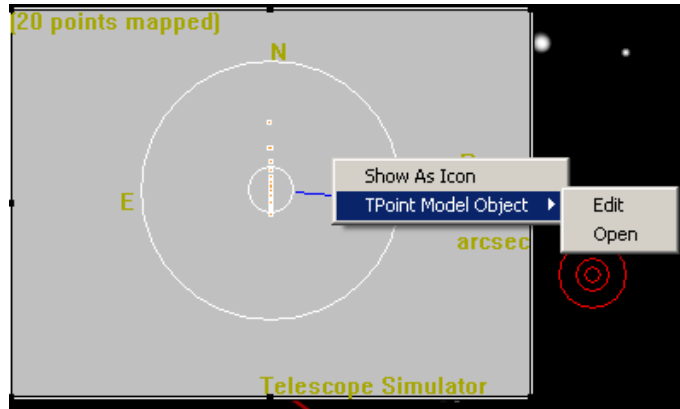
Pay close attention to the Sky RMS and the PSD along the top of this window. They are the most important numbers you need to watch throughout the process of selecting terms. As you can see in the picture below, the first six terms are already selected. Unless you have a really good reason to mess with these terms, **don't**. If you want to add terms other than these, the obvious thing to do is click on the **More Terms…** button like the one in the picture below. Clicking this button will bring up a whole list of new terms for you to include. Start by holding down the shift key and highlighting the TF, TX, HCES, HCEC, DCES, DCEC, DAF, DNP, IE, and IA terms and clicking the **use** checkbox. Then you can close this little window. Make sure the checkbox next to the Fork Flexure term is not checked, as in the photo above. The ROVOR scope doesn't even have a fork so it makes no sense to include this term. Now that you have included all of these terms, we need to keep the ones that helped the model and get rid of the
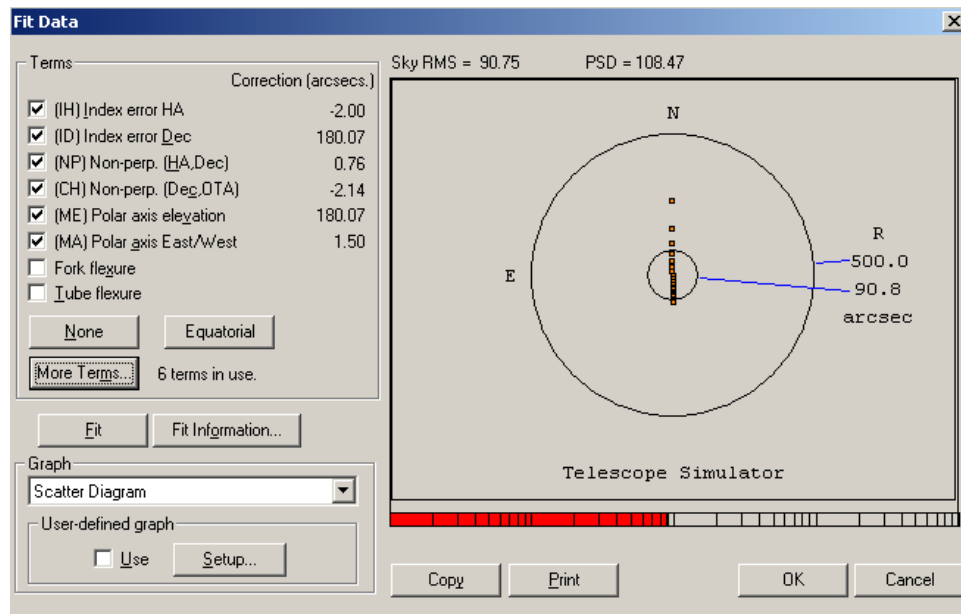
ones that hurt it. To do this, click on the **Fit Information…** button. This brings up the Fit Information dialogue box. This dialogue box just has a bunch of numbers in it, but they are some **very** important numbers. You will want to scroll down partway till you get a list of information like the one on the next page. Be careful: there is a very similar list of information at the very top of this dialogue box. We see three columns of numbers: the second two columns are the most important to us. The first lists the value, and the second lists the sigma. As you can see, the DAF term has a sigma that is large relative to its value. This means we should get rid of the DAF term. This brings our RMS from 71.47 to 71.10 and our PSD from 101.07 to 96.61. This is not a very big change in

RMS, but it did bring down the PSD, which is the real goal. In the above example, you will also notice that the CH term has a larger sigma than a value. This is a very bad situation, and you would normally want to get rid of any term like this. The only problem here is that the CH term is one of the

original six terms. You should not get rid of any of these six terms unless you know exactly what you are doing. The TPoint manual strongly suggests using the DAF term since our scope is has a Paramount ME mount. We have found this to be good advice.

After you throw out a term, you need to go back and look at the Fit Information again. Removing a term can really affect the value and sigma of the other terms. Terms that had a good value/sigma ratio before may not be worth a thing now. Also, the order in which you add or subtract terms can have an affect on the RMS. You will have to carefully select the terms that do the most for your RMS and PSD. Don't be afraid to play around with it a little bit. Another thing you will have to worry about is to make sure you have a large enough data set to justify all of the terms you are using. The larger your set, the more terms it will statistically support.

After you have chosen the terms you want to use, it is now time to consider adding statistical terms. These terms, also known as harmonic terms, are used to correct any harmonics that may be present in the data. The idea is to add terms that account for any sine or cosine trends that may be present in the data. You should read up on this on page 64 of the TPoint users manual. The easiest way to find harmonic terms is to
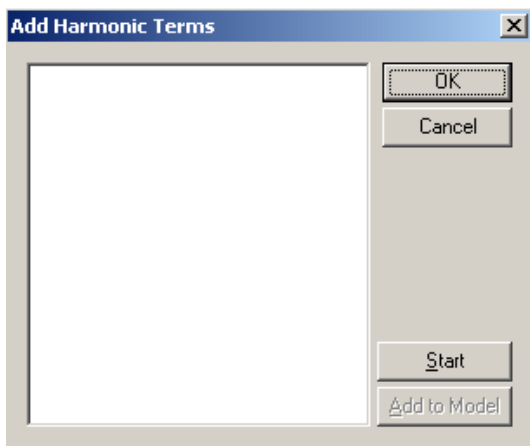
click on the **More Terms…** button and then click on the **Suggest Terms…** button. This brings up the screen to the left. Notice that it is empty. You will need to click on **Start** to get the search rolling. TPoint will give you a whole list of suggested terms. The names of the terms are given on the left of the screen, and then there are two columns of numbers. The first column is the RMS while the second is the PSD. These figures represent what the RMS and PSD will be if you choose to add that term to your model. The terms are organized with the best RMS and PSD first. You should be careful to select harmonic terms that lower the RMS and the PSD. 99% of these terms are not actually useful, and you won't want to include them: their RMS and PSD are worse than what

your current model uses.   If you see one or maybe two of these terms you want to include, highlight them and then click **Add to Model**.
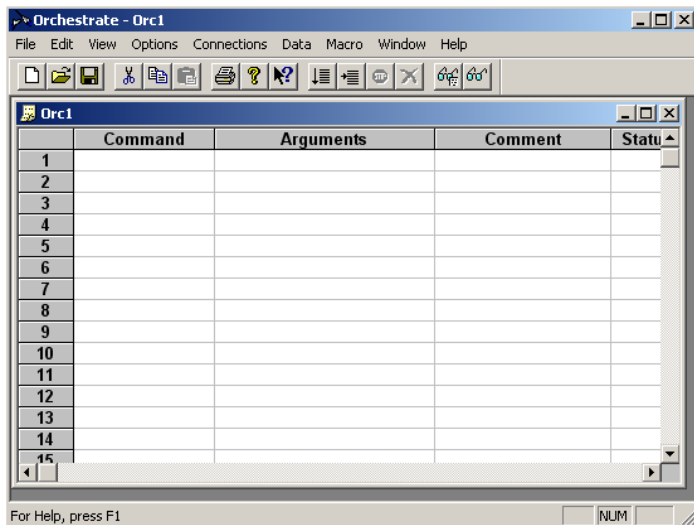
When you are finished, you should have a well understood model that accounts for the various mechanical imperfections of the mount. If your model just does what it does and you don't know why, then you really should do your homework. Your understanding of TPoint should not be limited to this article: please read up on the magic of TPoint in the TPoint manual.

How to use Orchestrate

This article is intended to help you understand how to use Orchestrate. It should not be a substitute for reading the Orchestrate manual. We will discuss the logic behind Orchestrate as well as some do's and don'ts.

❖ **What is Orchestrate?**

Orchestrate is a program that automates nearly all processes of controlling the telescope. Slewing (moving) the scope, adjusting the filter wheel, and controlling the camera are some of the core procedures that can be controlled by Orchestrate. Orchestrate accomplishes these tasks by telling TheSky6 how to move the scope and CCDSoft how to operate the camera and filter wheel. Orchestrate makes it possible to automate long observing sessions. You can create a script of commands, load it into Orchestrate, and let it run the show. Orchestrate also takes a lot of the sting out of making a TPoint model. Orchestrate's layout is similar to Excel, with columns for commands, arguments, comments, status, error messages

and so forth. In the Command column, you insert commands like SlewToRaDec or SetResolution. In the Arguments column you put modifiers necessary to complete the command. For example, SetResolution needs an argument to set the resolution, either High, Medium, or Low. You can enter helpful comments in the Comment column that will improve the readability of your script. The Status column gives you the status of the command. This column usually shows one of four things: a blank cell, indicating that the command has not yet been attempted: Done, indicating that the command successfully ran: Working…, indicating that the command is currently being executed: and error, which (obviously) tells you that an error occurred while attempting to execute that command. After the Status column comes the Error Msg column. This column gives a brief description of the error that occurred; it also gives you the error code. Looking up these error codes on the Internet can help you diagnose the reason why the command did not execute.

❖ **How do I use Orchestrate?**

As mentioned above, Orchestrate runs a series of commands, known as a 'script,' to make the telescope and camera do what you want them to do.   There are a few commands you will use over and over again. The most commonly used commands include SlewToRaDec, SlewToAzAlt, TakeImage, SetResolution, WaitFor, and AutoMap. Most of your scripts will consist of the repetition of some sort of slew command, a WaitFor command, and then an Image command. Different projects call for different scripts. When using Orchestrate to automate the process of gathering data points for a TPoint model, your first command will usually be

'SetResolution' with an argument of 'Medium.' The 'Medium' argument sets the bin rate to 2x2 'High' to 1x1, and 'Low' to 3x3. The 'AutoMap' command can work with images that were taken at a bin rate of 2x2: setting the resolution to medium will save you loads of time while gathering data points for a TPoint model. Also,

gathering data points for a TPoint model is best accomplished using the SlewToAzAlt command. If you are using the telescope for research, you will probably want the resolution set to 'High.' If you do not give Orchestrate a command to set the resolution, it automatically sets it to a 1x1 bin ratio.

Don't feel like you have to memorize all of these commands like in some CS class. There is a handy list of commands you can pull up. To access the command list, you must have an Orchestrate document open. Then go to **View | Command List**. You can highlight a cell in the Command column, then double click on one of the commands from the Command List to insert it into that cell. As mentioned earlier, all commands require some sort of modifier in the Arguments column for the command to run. After you insert a command into the command column, hit the right arrow or click in the cell in the Arguments column and insert your argument. See pages 11-12 of the Orchestrate pdf help file for a list of expected arguments.
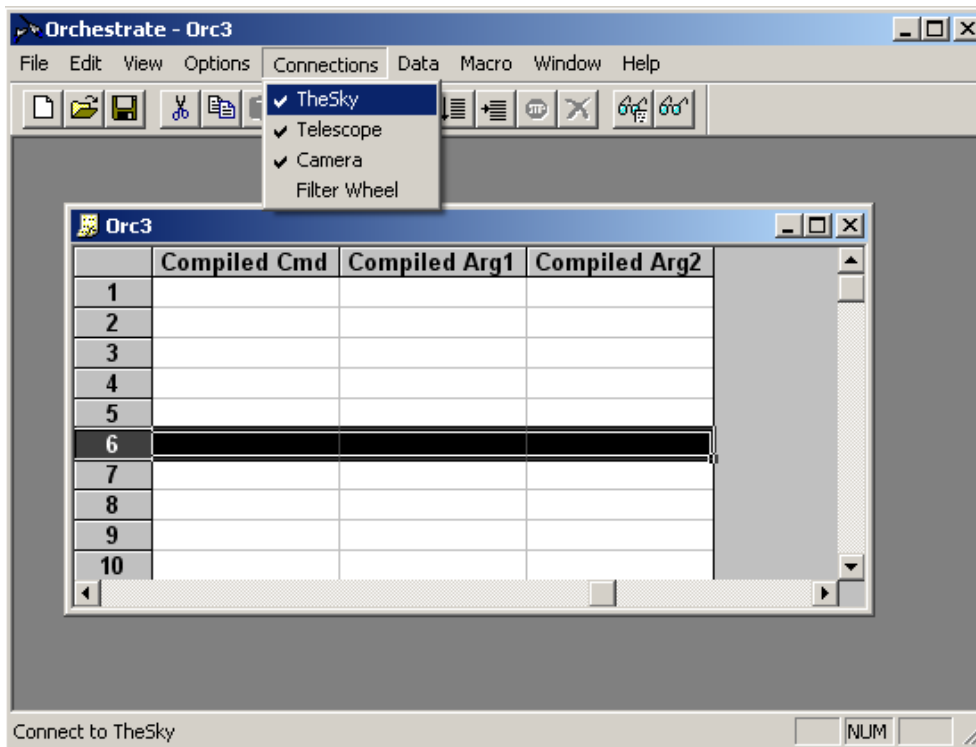
There are a few things you must do before attempting to use your script. First, make sure that Orchestrate is connected to TheSky6 as well as CCDSoft. Go to **Connections** to see the connections. Make sure TheSky6 and CCDSoft are open. Also be sure that TheSky6 has a connection to the telescope

and CCDSoft is connected to the camera and filter wheel. Next, click on all of the connections under the **Connections** menu to make the necessary connections. You should now be able to run your script.

Once you have completed your script and made the proper connections, now you need to try and run it. There are two buttons that will execute your script; one is **Step** and the other is **Run**. These buttons are found just below **Macro** on the toolbar. From left to right these buttons are Run, Step, Stop, and Abort. The **Stop** and **Abort** buttons are only available while Orchestrate is running a command. In other words, the stop and abort buttons are grayed out until you hit either the Run or Step button. The step command will only execute the currently highlighted command, and the run command will run the entire script. If you need to stop the script, hitting the stop button will stop the script after it finished the command it is currently working on. The abort button stops everything in its tracks: it is like the big red button on a band saw that you hit when you want it to stop right now.

Now it is time for some practice. You will have to know how to use Orchestrate to run a simulated telescope before you attempt to run the ROVOR telescope. The nice thing about this is that there is no danger of breaking a simulated telescope. The following exercises will guide you through the process of selecting commands and arguments, connecting to the simulated instruments, debugging and running your script. For help on encoding Arguments, be sure to look at pages 11-12 of the Orchestrate pdf help file.

(Read this entire section before beginning)
Your script should include commands to accomplish the following tasks
1. Set the camera resolution to medium.
2. Slew to the following targets in the order they are listed:
Sirius, RA: 05h 53m 33s Dec: -01d 35m 21s, NGC 1976, Azimuth:273d 32m 19s Altitude: -24d 26m 10s, M 78, RA: 04h 42m 25s Dec: +04d 19m 39s, Betelgeuse, Rigel
3. After slewing to each target, Wait for 2 seconds, then take a 10 second exposure.
4. Save your Orchestrate document as Exercise1 in
c:/Program Files/Sofware Bisque/Orchestrate/Scripts
5. Make the necessary connections in the Connections menu.
6. Run your script.

	Command	Arguments	Commen
1	SetResolution	Medium	
2	SlewToObject	Sirius	
3	WaitFor	2	
4	TakeImage	10	
5	SlewToRaDec	05h 53m 33s -01d 35m 21s	
6	WaitFor	2	
7	TakeImage	10	
8	SlewToObject	NGC1976	
9	WaitFor	2	
10	TakeImage	10	
11	SlewToAzAlt	273d32m 19s -24d 26m 10s	
12	WaitFor	2	
13	TakeImage	10	
14	SlewToObject	M78	
15	WaitFor	2	
16	TakeImage	10	
17	SlewToRaDec	04h 42m 25s +04h 19m 39s	
18	WaitFor	2	

Your Orchestrate document should look something like this.

A note on connections. Be sure that the telescope is set up as a simulator. In TheSky6, go to **Telescope |Simulator** and be sure the name is set to **Simulator.** For this practice exercise, you will also want to make sure that the "Impose slew limits" checkbox is unchecked. Similarly,

make sure CCDSoft is running a simulated camera. In CCDSoft, go to **Camera |Setup** and be sure it is set on **Simulator.**

After the SetResolution command, your script should be a repetition of three basic commands: a slew command, a Wait command, and a TakeImage command. If you mess up entering in the RA and Dec coordinates, it is impossible to go back and edit one of the values: you have to re-enter the entire string of coordinates. Also, if you want to insert a new command line between commands, click on the bottom command so it is highlighted, the go to **Edit |Insert** to insert the new command line.

One final note. In the above screenshot, you will notice that the argument for command number 17 has 04h 19m 39s as the Declination coordinates. This is different from the 04d 19m 39s that was specified in the problem. The SlewToRADec command expects the first Dec coordinate to be given in degrees, not hours. If you enter it in hours instead of degrees the telescope will not slew where you expect it to.

(Have a practice problem like 1.reproduce the following screen. One of the commands should give an error message 2.make all of the proper connections and execute your script 3.figure out what went wrong with the command that threw an error message, fix the problem, and execute the command again)

Index